AN ANATOMICAL BASIS FOR THE MANAGEMENT OF COMPLEX WRIST INJURIES

JAMES M MCLEAN, MB BS

Clinical Associate Lecturer

Discipline of Orthopaedics and Trauma

University of Adelaide, Australia

September 2009

Thesis by publication submitted for the degree of Master of Surgery, University of Adelaide.

APPENDIX 1

Watts AC, McLean JM, Fogg Q, Bain GI. **Scaphoid Anatomy**. In: Slutsky DJ, and Slade JF, ed. The Scaphoid. 1st ed. New York. Thieme Medical Publishers; 2009: *in press*.

Chapter 1: Scaphoid Anatomy

Authors: Adam C Watts MBChB[2]
James M McLean MBBS[3]
Quentin Fogg PhD [4]
Gregory I Bain PhD [1, 2]

Institutions:

1. Dept of Orthopaedics and Trauma, Royal Adelaide Hospital, Adelaide, South Australia, Australia.

2. Dept of Orthopaedic Surgery, Modbury Public Hospital, Modbury, South Australia, Australia.

3. Discipline of Orthopaedics and Trauma, The University of Adelaide, Adelaide, South Australia, Australia.

4. William Hunter Lecturer in Anatomy, The University of Glasgow, Glasgow, Scotland.

Watts, A.C., McLean, J.M., Fogg, Q. & Bain, G.I. (2009) 'Scaphoid Anatomy', in Slutsky, D.J. & Slade, J.F. (eds), The Scaphoid, 1st ed, New York, Thieme Medical Publishers, *in press*.

APPENDIX 2

Imaging Recognition of Morphological Variants at the Midcarpal Joint

SCIENTIFIC ARTICLE

Imaging Recognition of Morphological Variants at the Midcarpal Joint

James M. McLean, MBBS, Gregory I. Bain, PhD, Adam C. Watts, MBChB, Luke T. Mooney, MBBS, Perry C. Turner, MBChB, Mary Moss, MBBS

Purpose To compare the imaging methods for identifying the various morphological variations of the articular surfaces at the midcarpal joint.

Methods Thirteen cadaveric wrists were examined by plain neutral anteroposterior radiographs; 2-dimensional computed tomography (CT); 3-dimensional CT reconstruction, and 3-tesla magnetic resonance imaging (MRI). Carpal measurements were performed, and the parameters that defined the scaphoid, lunate, hamate, and capitate morphological types were investigated, with dissection being used as the definitive measure of morphology. The dissection findings were compared to the results of each imaging technique to determine the accuracy of morphological determination from each technique.

Results Lunate type was the most accurately identified morphological variant amongst all imaging techniques. Lunate type was most accurately determined from coronal MRI. A lunate with a small, cartilaginous ulnar facet (intermediate type) could be differentiated only by coronal MRI and dissection. Scaphoid type could not be determined accurately using any of the imaging modalities described. Capitate type was most accurately determined from coronal MRI. However, flat and spherical-type capitates could not be routinely differentiated from V-shaped capitates. Hamate type was most accurately determined from 3-dimensional CT reconstruction.

Conclusions Accurate identification of carpal bone morphology is required to improve our understanding of carpal mechanics and pathology. Not all morphological features can be identified radiographically. Direct visualization is required to differentiate types of scaphoid, and to differentiate V-type capitates. MRI provides the most accurate identification of lunate type, and 3-dimensional CT provides the best method of differentiating hamate types. *(J Hand Surg 2009;34A:1044–1055. © 2009 Published by Elsevier Inc. on behalf of the American Society for Surgery of the Hand.)*

Key words Midcarpus, wrist, x-ray, computed tomography, magnetic resonance imaging.

Additional material is available online.

A DETAILED KNOWLEDGE OF the fundamentals of carpal anatomy is integral to our understanding of carpal mechanics and pathomechanics, because these principles form the basis to formulate efficacious treatment plans that are anatomically and mechanically sound.[1,2] Successful diagnosis of wrist injuries, the interpretation of images, and subsequent management of disorders depend on accurate knowl-

From the Discipline of Orthopaedics and Trauma, The University of Adelaide, Adelaide, South Australia; Department of Orthopaedics and Trauma, Royal Adelaide Hospital, Adelaide, South Australia; Department of Orthopaedic Surgery, Modbury Public Hospital, Modbury, South Australia; Department of Radiology, Royal Adelaide Hospital, Adelaide, South Australia.

Received for publication November 22, 2008; accepted in revised form March 3, 2009.

Financial support was received from the Royal Australasian College of Surgeons (RACS), including an RACS Foundation W. G. Norman Research Scholarship, and from the Modbury Public Hospital Foundation, including a research grant, for Dr. James McLean while he undertook a Masters of Surgery at the University of Adelaide, Adelaide, South Australia, Australia.

Corresponding author: Gregory I. Bain, PhD, 196 Melbourne Street, North Adelaide 5006 SA, Australia; e-mail: greg@gregbain.com.au.

0363-5023/09/34A06-0010$36.00/0
doi:10.1016/j.jhsa.2009.03.002

edge of the morphological variations of the wrist and particularly how these variations relate to variations in soft tissue orientation and pathomechanics.[3]

There is little in the current literature to address noninvasive imaging identification of the midcarpal anatomical variants, and no standard exists for accurate recognition of these variants by different imaging techniques. This has limited the development in understanding of carpal kinematics and pathomechanics and any differences that might be related to these variations in morphologic features. Before a comprehensive investigation of carpal morphology can be undertaken, a clear standard for identification of these morphological variants must be established. The purpose of this study was to evaluate the best method for noninvasive imaging identification of the various morphological variations of the articular surfaces at the midcarpal joint. The articular surfaces under investigation included the distal scaphoid, the distal lunate, the triquetral hamate opposing surfaces, and the proximal capitate.

MORPHOLOGICAL VARIATIONS OF THE ARTICULAR SURFACES AT THE MIDCARPAL JOINT

The distal articular surface of the scaphoid at the scaphotrapezium-trapezoid (STT) joint has been reported to have a variable inter-facet ridge that divides the surface into 2 articular facets, corresponding to the direction of trapezio-trapezoidal articulation.[4–9] Moritomo et al. suggested that the presence or absence of this ridge might indicate a clear pattern of scaphoid motion relative to the trapezio-trapezoidal joint.[10]

Viegas et al. classified 2 types of lunate based on the midcarpal distal articulation of the lunate, as alluded to by previous investigators.[4,11–16] In this description, a type I lunate has a single distal facet for the capitate, and it does not articulate with the hamate. In contrast, a type II lunate has 2 distal facets: the radial facet articulates with the capitate, and the ulnar facet articulates with the hamate. Differences in lunate type have been reported to be associated with variations in ligament composition and distribution,[3,17–19] carpal kinematics[20,21] and pathomechanics,[22] and various carpal pathologies.[3,13,17,23–25]

McLean et al.[26] described 2 distinct patterns of triquetrum-hamate (TqH) joint, with a spectrum of variation between them. In this study, 2 distinct patterns of hamate articular surface were identified. At 1 end of the spectrum, the hamate possessed a prominent groove that formed a ridge distally. This configuration formed a helicoidal TqH joint composed of double-faceted, complementary concave and convex parts. At the other end of the spectrum, the hamate possessed no hamate groove or distal ridge, and it formed a joint that was predominantly oval convex.

Yazaki et al.[27] recently described 3 types of capitate based on the articulating surface of the capitate head, as alluded to by Viegas.[13] In this description, a flat (F-type) capitate was characterized by a horizontal lunate articulation and a nearly vertical scaphoid articulation. A V-shaped (V-type) capitate had separate lunate and scaphoid facets that converge and were separated by a visible capitate ridge, corresponding to the direction of the scapholunate joint. A spherical (S-type) capitate had an associated concave articulation formed by the scaphoid and lunate facets. The capitate head corresponded to the shape of the capitate facet of the scaphoid. Variations in the concavity of the scaphoid facet for the capitate have been identified,[7,28,29] with the facet ranging from shallow to deeply convex.[6,7,14,20,29–31] It has been suggested that differences in capitate type are likely to be associated with variations in ligament composition and distribution, differences in carpal kinematics and pathomechanics, and variations in surgical outcomes, such as proximal row carpectomy.[27]

MATERIALS AND METHODS

Thirteen unilateral adult human wrists were collected from embalmed cadavers. The mean age at death was 82 years (range 64–94). Seven were male, and 6 were female. The specimens were derived from arms cut through the mid-portion of the humerus. All analyzed imaging variables were measured and recorded by 2 observers who were blinded to the results of the cadaveric dissection. The measurements were done independently on 2 separate occasions at a minimum of a week apart. Intra- and inter-observer kappa statistics were performed to assess agreement using the method of Landis and Koch.[32]

Imaging parameters

Plain radiographs: Plain anteroposterior (AP) radiographs were taken of each specimen. The dorsum of the hand was held flat against the radiographic cassette. A customized jig was used to hold the specimens with the wrist in neutral radioulnar deviation, maintaining the straight alignment of the long finger metacarpal, capitate, and radius. All plain wrist radiographs were analyzed using a Samsung 3072 × 3072 (9.4 megapixels) RAYPACS Display Workstation (Samsung SDS Co., Ltd, Korea) and IMPAX 6.0 software (IMPAX, Agfa HealthCare NV, Mortsel, Belgium).

Computed tomography: The specimens were then imaged in a standard computed tomography (CT) scanner (Aq-

uilion 16; Toshiba Medical Systems Inc., New York, NY) using the same customized jig to hold the specimens, and using a technique of 120 kV, 80 mA, with 0.5-second rotation. This generated an average of 600 contiguous slices, 0.5 mm thick, with a reconstruction interval of 0.3 mm, from approximately 30 mm proximal to the carpus to approximately 30 mm distal to the carpus. All the images were analyzed using a Flexscan L885 Viewer (Eizo Nanao Technologies Inc, Cypress, CA), with Vitrea 2, version 3.8 software (Vital Images Inc, Minnetonka, MN). The magnification function supplied with the standard CT scanner software was used in conjunction with re-centering of the area of interest and subsequent magnification of the image up to 10 times. The contiguous 2-dimensional images were analyzed in the coronal, sagittal, and transverse planes before being imported into the 3-dimensional surface reconstruction program. Before 3-dimensional reconstruction, portions of the original 2-dimensional CT images were selectively erased in order to eliminate structures obscuring or overlying the elements of interest. An edge-sharpening bony algorithm was empirically chosen to yield high resolution of bony detail. Using the bone removal package, we isolated individual bones from the remainder of the surrounding osseous structures, by mathematical disarticulation using the commercial bony algorithm. This facilitated assessment of the morphological parameters being investigated (Video 1; this video can be viewed at the *Journal's* Web site, www.jhandsurg.org).

Magnetic resonance imaging: The specimens were then imaged in a 3-tesla Siemens Tim TRIO magnetic resonance imaging (MRI) scanner (Siemens Medical, Erlangen, Germany) with each cadaver wrist placed palm down and held in a MEDRAD 8-channel wrist array (MEDRAD Inc., Warrendale, PA). Commercial sequences of Syngo B15 software were used, with single-quantum gradients of 40 mT/m and saturation recovery 200 mT/m/ms (Syngo MR 2004A, MAGNETOM Symphony; Siemens Medical Solutions Inc., Malvern, PA). A 3-dimensional image volume was obtained with a gradient-echo technique, using a coronal 0.4-mm isotropic 3-dimensional dual-echo steady-state sequence. The imaging parameters for the gradient-echo sequence were as follows: field of view, 100 × 100 mm; matrix, 256 × 243; section thickness, 0.5 mm; 112 contiguous slices; prescan normalized, receiver bandwidth 283 Hz/pixel; flip angle 30°; repetition time ms/echo time ms = 12.95/4.12. When these parameters were used, the voxel size was 0.4 × 0.4 × 0.4 mm. The imaging time for the volume acquisition was approximately 4.17 minutes per wrist.

Dissection

The specimens were then dissected under 2.5× loupe magnification, using a dorsal approach to expose the midcarpal joint. The skin, subcutaneous tissues, and extensor tendons were excised, and the joints were inspected. Dissection was used as a definitive measure of the morphological parameters being investigated. Differentiation of morphological variants was determined at the time of dissection by the consensus of 2 observers. The presence or absence of degenerative changes was observed at the midcarpal joint. An electronic digital caliper was used to measure pertinent morphological parameters. Photographs of the specimens were taken using a tripod-mounted digital camera (6.24 Nikon D70 SLR, Nikon Australia Pty. Ltd., Sydney, N.S.W., Australia). All photographs taken were of right wrists. The dissection findings were compared to the results of each imaging technique to determine the accuracy of assessment of the morphologically different carpal bones.

Identification of carpal morphological types

The parameters that defined the scaphoid, lunate, capitate, and hamate types were observed to be either visible or not visible on analysis for each imaging modality.

Scaphoid type: The distal scaphoid articular surface at the STT joint was identified as having either a smooth, articulating surface or a scaphoid ridge that marked the division of the distal scaphoid into a double-faceted articulating surface, for articulation with the trapezium and trapezoid, respectively.[3,5] A smooth, articular surface was categorized as type 1 (Fig. 1A), and a double-faceted surface was categorized as type 2 (Fig. 1B).

Lunate type: The midcarpal lunate articular surface was identified as having either a single or a double articulating facet. A single midcarpal facet was defined as a type I lunate (Fig. 2A), and a double articulating facet was defined as a type II (Fig. 2B).[12,13] Measurements of capitate–triquetrum distance (C-T distance) and the lunate ulnar facet were made using the image-specific software and digital calipers. The C-T distance was measured with the wrist in neutral radioulnar deviation, maintaining the straight alignment of the middle finger metacarpal, capitate, and radius. Nakamura et al. reported that the shortest distance between the capitate and triquetrum (C-T distance) was the best determinant of lunate type, and that the C-T distance increased as the actual width of the lunate ulnar facet increased.[33]

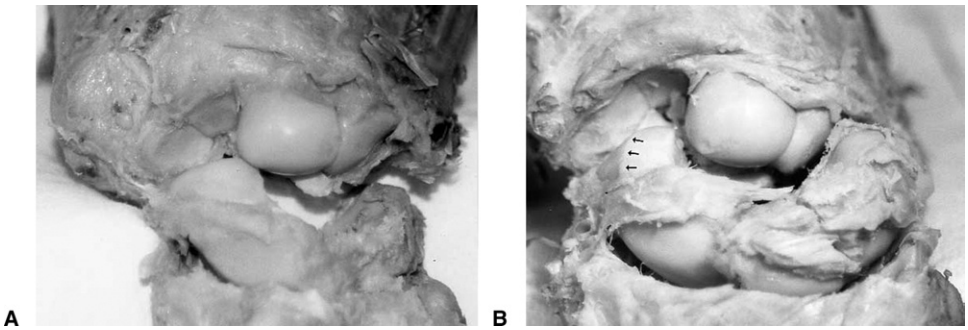

FIGURE 1: The dissected specimen has been opened dorsally to expose the midcarpal and radiocarpal joints. **A** A type 1 scaphoid in which the distal articular surface of the scaphoid surface is smooth and flat. **B** A type 2 scaphoid, displaying the distal articular surface of the scaphoid, which is double-faceted, with a clear ridge corresponding to the direction of trapezio-trapezoidal articulation. (Reprinted with permission from Viegas SF. Variations in the skeletal morphologic features of the wrist. Clin Orthop Relat Res 2001;383:21–31).

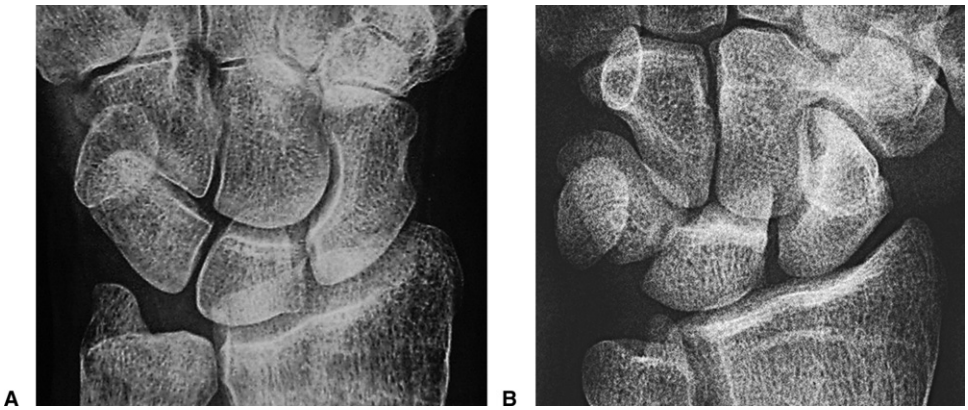

FIGURE 2: A plain AP radiograph of the wrist. **A** A type I lunate with a single distal facet for the capitate. A type I lunate does not articulate with the hamate. There is evidence of STT osteoarthritis. **B** A plain AP radiograph of a type II lunate with a large lunate facet.

Nakamura et al. defined type I lunates as those having a C-T distance of <2 mm and type II lunates as those having a C-T distance of >4 mm.[20]

Hamate type: The hamate was analyzed for the presence or absence of the hamate groove and distal hamate ridge on its midcarpal surface. A type I hamate was defined as possessing no hamate groove or distal ridge (Fig. 3A).[26] The presence of a groove and a distal ridge was defined as a type II hamate (Figs. 3B, 4).[26]

Capitate type: The capitate head was categorized using the descriptions of Yazaki et al.[27] A capitate with a horizontal lunate articulation and a nearly vertical scaphoid articulation was defined as an F-type capitate (Fig. 5). A capitate with separate lunate and scaphoid facets that converge to form a ridge (capitate ridge) was defined as a V-type capitate (Fig. 6). An S-type capitate was defined as a capitate with predominantly convex shape, with complementary concave articulation formed by contiguous smooth facets of the scaphoid and lunate (Fig. 7). The diameter of the capitate head was measured using the image-specific software and digital calipers. Nakamura et al. reported that the radius of the capitate head was statistically smaller when associated with type II lunate wrists.[20]

Statistical analysis

For inter-observer and intra-observer agreement studies, the alpha value was set at 5%. Statistical comparison of agreement was performed according to the methods of Bland and Altman.[34] Degree of agreement was categorized according to Landis and Koch.[32]

Correlation coefficients, sensitivity, specificity, positive predictive value, negative predictive value, and accuracy were determined by construction of 2 × 2 tables for the investigations that demonstrated observer agreement.[35] Findings at cadaveric dissection were taken as the reference standard for accuracy calculations.

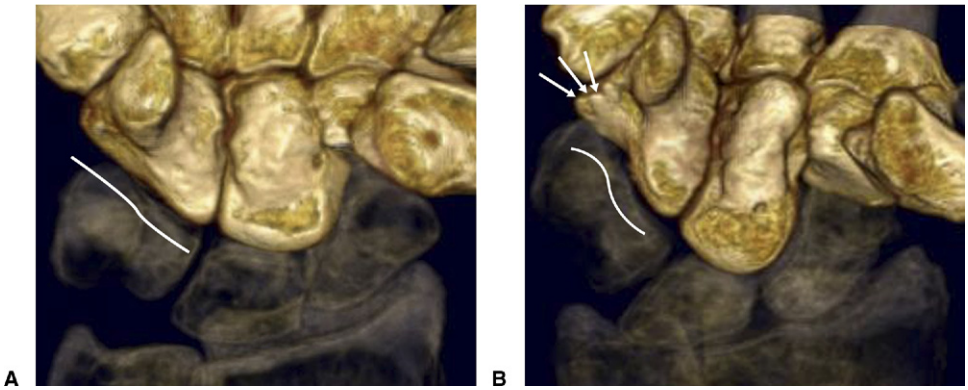

FIGURE 3: Three-dimensional volar reconstructions of the carpus. The proximal row is represented by semitransparent osseous elements. Three-dimensional reconstruction allows 360° visualization of the osseous elements being investigated. **A** The absence of a groove at the triquetro-hamate joint is characteristic of a type I hamate. **B** In comparison, the spiral configuration of the hamate groove is well visualized with this modality and is typical of a type II hamate.

FIGURE 4: A 3-dimensional ulnar reconstruction of the carpus. The triquetrum and pisiform have been disarticulated from the hamate and are represented by the semitransparent osseous elements overlying the hamate. The spiral configuration of the hamate groove is well visualized in this projection, as well as the distal ridge that is typical of a type II hamate.

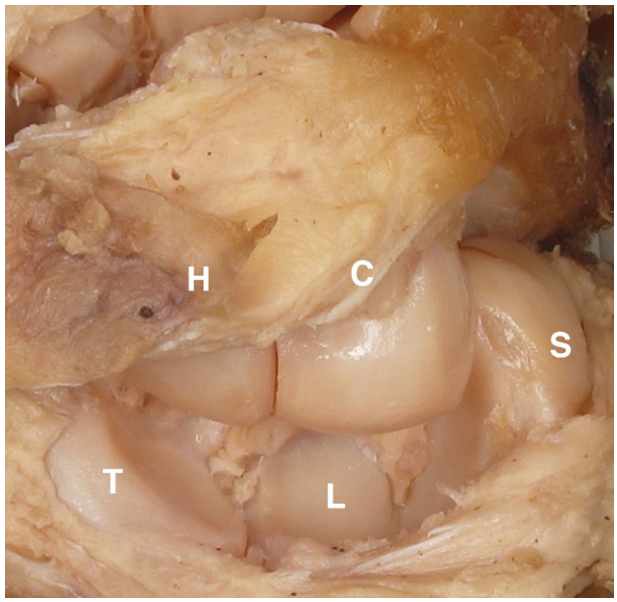

FIGURE 5: Dissected specimen of the midcarpal joint opened dorsally, showing a flat type (F-type) capitate. It is characterized by a horizontal lunate articulation and a nearly vertical scaphoid articulation. C, capitate; H, hamate; L, lunate; S, scaphoid; T, triquetrum. (Reprinted from Yazaki N, Burns ST, Morris RP, Andersen CR, Patterson RM, Viegas SF. Variations of capitate morphology in the wrist. J Hand Surg 33A,660–666, with permission from Elsevier.)

RESULTS

Plain neutral anteroposterior radiographs

In the neutral AP view, the scaphoid was positioned in slight rotation with a variable degree of flexion. In this projection, the trapezoid and trapezium appeared superimposed over the distal scaphoid, making analysis of the STT joint difficult (Figs. 2A, 2B). In those specimens with associated STT osteoarthritis (3/13, 23%), joint narrowing further limited assessment of the joint (Fig. 2A).

In the AP view, the distal lunate was variably superimposed over the proximal capitate head. This made differentiating small ulnar facets difficult, especially when combined with the normal slight rotation of the lunate. The lunate type was easily visualized with large ulnar facets (5/5, 100%) (Fig. 2B).

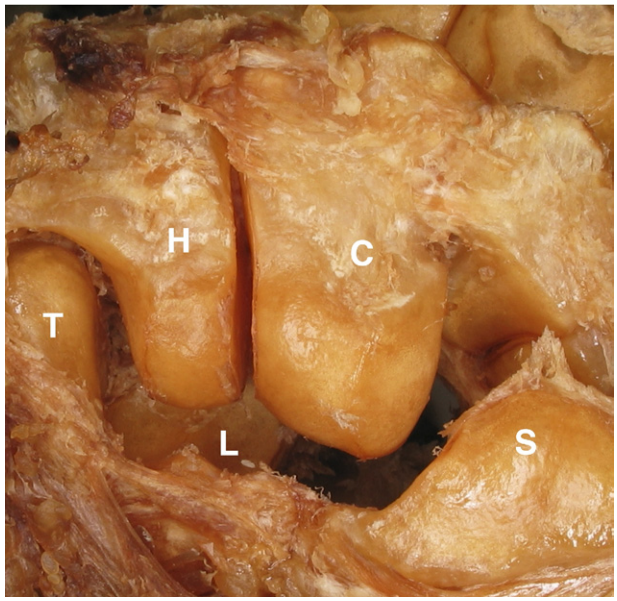

FIGURE 6: Dissected specimen of the midcarpal joint opened dorsally, showing a V-shaped (V-type) capitate. It is characterized by separate lunate and scaphoid facets that converge, separated by a visible ridge, corresponding to the direction of the scapholunate joint. C, capitate; H, hamate; L, lunate; S, scaphoid; T, triquetrum. (Reprinted from Yazaki N, Burns ST, Morris RP, Andersen CR, Patterson RM, Viegas SF. Variations of capitate morphology in the wrist. J Hand Surg 2008;33A:660–666, with permission from Elsevier.)

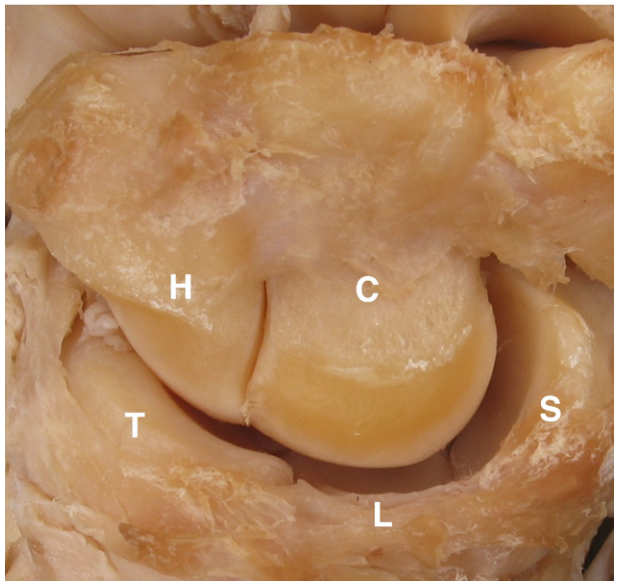

FIGURE 7: Dissected specimen of the midcarpal joint opened dorsally, showing a spherical (S-type) capitate. It is characterized by a round capitate head, with an associated concave articulation formed by the scaphoid and lunate facets. C, capitate; H, hamate; L, lunate; S, scaphoid; T, triquetrum. (Reprinted from Yazaki N, Burns ST, Morris RP, Andersen CR, Patterson RM, Viegas SF. Variations of capitate morphology in the wrist. J Hand Surg 2008;33A: 660–666, with permission from Elsevier).

In the neutral AP view, the triquetrum and pisiform sat variably superimposed over the articulating surface of the hamate, making analysis of the triquetro-hamate joint difficult (Figs. 2A, 2B). The spiral shape of the hamate groove was poorly visualized, and the distal ridge could not be routinely identified owing to the difficulty in differentiating it from surrounding and overlying osseous structures.

In the AP projection, the scaphoid and lunate sat superimposed over the capitate head (Figs. 2A, 2B). When present, the capitate ridge was difficult to visualize, as its direction corresponded to the direction of the scapholunate joint, and it was well visualized only when the projection was perfectly aligned with the scapholunate joint. This made differentiating the surface structure of the capitate head difficult.

Computed tomography imaging

The scaphoid ridge could not be identified in the transverse, sagittal, or coronal planes on CT. A large single or double facet of the lunate could be accurately identified on the coronal plane CT slices. However, CT imaging could not routinely differentiate lunates with small, cartilaginous facets from type I lunates. Computed tomography imaging using transverse and sagittal planes was not useful in the identification of hamate variants. The distal ridge could be identified in the coronal plane, but its nonlinear course made it difficult to differentiate from surrounding structures in some images. Although the concavity that represented the hamate groove could be visualized in the coronal plane, its spiral course made differentiation difficult. The capitate ridge and shape of the head could be assessed on coronal plane CT slices only.

3-dimensional computed tomography imaging

The bony algorithm did not routinely differentiate between scaphoid, trapezoid, and trapezium. This made mathematical disarticulation of the scaphoid from the trapezium and trapezoid difficult, despite meticulous bone remodeling. Consequently, it was not possible to routinely isolate the scaphoid distal surface in order to accurately determine whether there was a smooth single or double facet.

Although mathematical disarticulation of the capitate and hamate from the lunate was more straightforward, the lunate surface was difficult to interpret after it was isolated. The cartilaginous chondral surface was removed

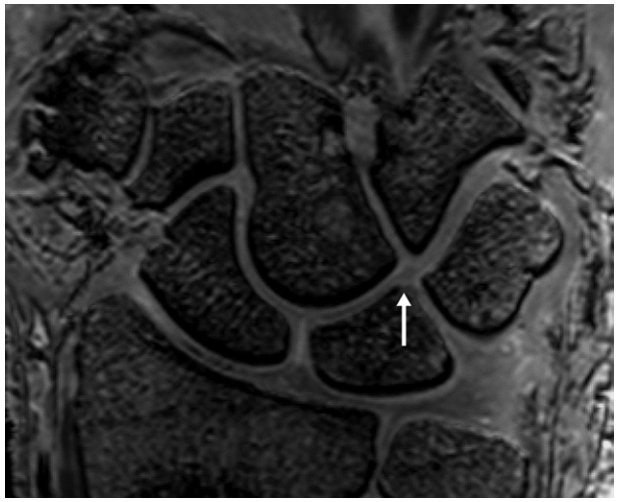

FIGURE 8: A coronal MRI of the wrist, showing a small, cartilaginous ulnar lunate facet for articulation with the hamate. The capitate has a spherical appearance typical of the S-shaped type capitate.

by the bony algorithm, which produced an uneven surface that lacked the resolution to accurately determine a single or double facet. Consequently, it was not possible to routinely determine lunate type using this technique.

With the hamate, the presence of the spiral groove and distal ridge could be visualized clearly after the overlying osseous elements were removed. Relatively accurate interpretation of type I (Fig. 3A) and type II (Figs. 3B, 4) was possible.

The bony algorithm did not routinely differentiate between scaphoid and capitate. This made mathematical disarticulation of the scaphoid from the capitate difficult, despite meticulous bone remodeling. In addition, after it was isolated, the capitate surface was difficult to interpret, as the predominantly cartilaginous capitate ridge had been removed (Figs. 3A, 3B). This produced a rounded surface that lacked the resolution to accurately determine capitate type.

Magnetic resonance imaging

The scaphoid ridge and lunate facets could not be identified in the transverse or sagittal cuts. Although the scaphoid ridge could be identified in the coronal plane, this could not be achieved routinely (2/13, 15%). In those specimens with a visible ridge, the ridge appeared to be entirely cartilaginous and to form part of the chondral surface.

Lunates with a large single or double facet could be identified on coronal plane MRI cuts. From these images, it was possible for observers to routinely differentiate lunates with small cartilaginous ulnar facets from type I lunates (Fig. 8).

The hamate groove could be visualized in coronal plane MRI slices, but its spiral course made differentiation difficult. The distal ridge was better visualized from soft tissue using coronal MRI compared to coronal CT, but similarly, its nonlinear course made it difficult to differentiate. The capitate ridge and shape of the head could be assessed in the coronal plane (Fig. 8).

Cadaveric anatomy

The surface of the scaphoid was examined to differentiate scaphoid types. Five of 13 (38%) had a smooth distal scaphoid surface (type 1; Fig. 1A), and 8 of 13 (62%) were double-faceted (type 2; Fig. 1B). Two of 5 (40%) type 1 and 2 of 8 (25%) type 2 showed evidence of cartilage erosion at the STT joint with exposed chondral bone.

Five of 13 lunates dissected (38%) were type I (Fig. 2A) and 8 of 13 (62%) were type II (Fig. 2B). Of the type II lunates, 2/13 (15%) had a small cartilaginous volar-ulnar facet confirmed by MRI (Fig. 8). Three of 8 (38%) of the type II lunates had associated arthritis of the luno-hamate joint, whereas 0/5 (0%) of the type I lunates had arthritis. Two of 13 (15%) of the specimens had a rupture of the scapholunate ligament, both of which were present in wrists with type I lunates. The average C-T distance and ulnar facet width for each technique is presented in Table 1. In those specimens with a small ulnar facet identified at dissection, the MRI and CT images were examined to confirm cartilaginous-only ulnar facets.

On dissection, the hamate groove could be visualized and recorded. The distal ridge was not readily visible because it was covered by capsular and ligamentous attachments. Some specimens required additional dissection of the overlying soft tissue to allow accurate visualization of the hamate ridge. Seven of 13 (54%) were type I hamates (Fig. 3A) and 6/13 (46%) were type II (Figs. 3B, 4). One of 7 (14%) type I and 3/6 (50%) type II showed evidence of cartilage erosion with exposed subchondral bone at the hamate articular surface.

The capitate ridge could be visualized on dissection. Five of 13 (38%) were F-shaped (Fig. 5), 2/13 (16%) were V-shaped (Fig. 6), and 6/13 (46%) were S-shaped (Fig. 7). All specimens had a capitate ridge of varying prominence that corresponded to the direction of the scapholunate articulation.

Imaging studies

Table 2 summarizes the results of intra-observer and inter-observer agreement of categorization of carpal

TABLE 1. Measurement of Lunate Morphology

	Type I Lunate Group	Lunates With Small, Cartilaginous Ulnar Facets (Type III)	Type II Lunate Group, Not Inclusive of Lunates With Small, Cartilaginous Ulnar Facets	Type II Lunate Group, Inclusive of Lunates With Small, Cartilaginous Ulnar Facets	Total
Mean C-T distance (mm)	2.50 (SD: 1.05) (R: 0.70–3.65)	2.68 (SD: 0.49) (R: 2.20–3.18)	5.57 (SD: 1.22) (R: 3.30–7.09)	4.84 (SD: 1.67) (R: 2.20–7.09)	3.95 (SD: 1.85) (R: 0.70–7.09)
Mean ulnar facet width measured on CT (mm)	—	2.57 (SD: 0.40) (R: 2.13–3.01)	4.69 (SD: 0.60) (R: 3.37–5.43)	4.16 (SD: 1.09) (R: 2.13–5.43)	4.16 (SD: 1.09) (R: 2.13–5.43)
Mean ulnar facet width measured on MRI (mm)	—	1.79 (SD: 0.05) (R: 1.75–1.87)	4.14 (SD: 0.50) (R: 3.44–5.05)	3.54 (SD: 1.12) (R: 1.75–5.05)	3.54 (SD: 1.12) (R: 1.75–5.05)
Mean ulnar facet width measured at dissection (mm)	—	1.79 (SD: 0.07) (R: 1.67–1.87)	4.20 (SD: 0.45) (R: 3.76–5.16)	3.59 (SD: 1.13) (R: 1.67–5.16)	3.59 (SD: 1.13) (R: 1.67–5.16)

type for each imaging modality. Table 3 summarizes the relative accuracy of each imaging technique in the identification of midcarpal morphological variants. If there was no observer agreement (kappa value < 0), accuracy was not calculated.

DISCUSSION

Our understanding of normal morphological variants of the carpal bones and the relationship of these variations to carpal kinematics is improving, and accurate identification of these variations might influence management and outcome of treatment. Although many morphological characteristics can be visible at arthroscopy or arthrotomy, it is preferable to be able to gain an accurate understanding of the anatomy before surgery in order to aid preoperative planning and to direct treatment. Radiological methods including plain radiographs, CT, and MRI offer noninvasive, repeatable investigations that can be used both clinically and as research tools.

Scaphoid

The morphology of the distal scaphoid surface at the STT joint could be accurately determined only at dissection. The incidence of type I (smooth) scaphoid reported in this study was 38%, which was higher than previous studies (10–19%).[3,5,6,19] However, half of these specimens had osteoarthritis at the STT joint, as wrists with degenerative changes were not excluded from this study. This factor might affect our ability to classify accurately some aspects of the anatomy, and it deserves consideration in future investigations. Clinically, this finding would suggest that scaphoid type can be determined only at arthroscopy with visual inspection of the distal scaphoid STT articular surface.

Magnetic resonance imaging indicated that the ridge was primarily cartilaginous and, consequently, it could not be routinely identified by any radiographic technique. This finding was supported by previous histological studies that demonstrated that the ridge is cartilaginous and likely to be formed as a consequence of linear motion at the STT joint.[31] This suggestion is contrary to previous studies by Moritomo et al. that suggested that the ridge restricted the motion of the scaphoid against the trapezium and trapezoid, implying that the ridge was capable of resisting mechanical strain, particularly rotation of the scaphoid.[10] The authors support the view that the ridge is formed as a consequence of linear motion at the STT joint and is not

TABLE 2. Intra- and Interobserver Agreement (kappa) Statistics for Each Carpal Bone and Method of Imaging

Bone	Imaging	Intraobserver Kappa	p	Interobserver Kappa	p
Scaphoid	X-ray	<0	.308	<0	.429
	CT	<0	.853	<0	.853
	3-D CT	<0	.725	<0	.429
	MRI	<0	.853	0.05	.853
Lunate	X-ray	1.00	.001	1.00	.001
	CT	0.85	.002	0.85	.002
	3-D CT	0.85	.002	0.85	.002
	MRI	1.00	.001	1.00	.001
Hamate	X-ray	<0	.026	<0	.170
	CT	<0	.391	<0	.797
	3-D CT	0.85	.002	1.00	.001
	MRI	<0	.853	<0	.170
Capitate	X-ray	<0	.700	<0	.619
	CT	0.38	.170	0.38	.170
	3-D CT	<0	.414	<0	.107
	MRI	0.63	.002	0.51	.006

<0, no agreement; 0–0.2, slight agreement; 0.21–0.4, fair agreement; 0.41–0.6, moderate agreement; 0.61–0.8, substantial agreement; 0.81–1.0, almost perfect agreement.[30]

X-ray, plain AP radiographs; 3-D CT, 3-dimensional computed tomography.

TABLE 3. Accuracy of the Imaging Techniques for Identification of Morphological Variants Where Some Observer Agreement Was Demonstrated[33]

Bone	Imaging	Sensitivity	Specificity	PPV	NPV	Accuracy
Lunate	X-ray	1.00	0.88	0.83	1.00	0.92
	CT	1.00	0.75	0.71	1.00	0.85
	3-D CT	1.00	0.75	0.71	1.00	0.85
	MRI	1.00	1.00	1.00	1.00	1.00
Hamate	3-D CT	1.00	0.86	0.86	1.00	0.92
Capitate	CT	0.90	0.40	0.69	0.40	0.69
	MRI	0.90	0.65	0.65	0.90	0.82

PPV, positive predictive value; NPV, negative predictive value; X-ray, plain AP radiographs; 3-D CT, 3-dimensional computed tomography.

a factor influencing motion.[31] Consequently, the presence or absence of the ridge might be an indicator of motion pattern of the scaphoid relative to the trapezium and trapezoid.

Nuttal et al. have previously suggested that an STT arthrodesis undertaken in a wrist with nonlinear scaphoid motion wrist might result in a greater loss of movement than a wrist with linear scaphoid motion, and hence explain some of the unexpected adverse surgical outcomes reported in the literature.[8] In a wrist with a ridge (suggestive of linear motion at the STT joint), the surgeon might consider other surgical options in preference to STT arthrodesis in these patients.

Lunate

The incidence of type I lunates reported in this study was 38%, which was similar to previous radiographic and larger cadaveric studies (27% to 34.5%),[3,12–14,17,23,24,36] and lower than previous MRI studies (42.5% to 50%).[25,37] The results of

this study suggested that the morphology of the lunate can be accurately determined only by combined MRI imaging and visualization at arthroscopy or dissection. Although large lunate facets could be routinely identified by plain AP radiographs and coronal CT scans, lunates with small, cartilaginous facets were identifiable only with either coronal MRI (Fig. 11) or dissection. This finding supports previous investigations that reported that small ulnar facets were not always identifiable on plain radiographs[12,13,17,20,24,38] or on coronal CT images.[39]

Cartilage erosion with exposed chondral bone at the proximal pole of the hamate was evident at dissection in 38% of the type II lunates, which was consistent with previous studies (28% to 44.4%).[3,12–14,17,23–25,36,37] None of the type I lunates had hamate arthritis, which was also consistent with previous studies (0–4.1%).[3,12–14,17,23–25,36] Type II lunates have been found to have a greater incidence of arthritis[13,17,23–25] and chondromalacia[3] at the luno-hamate joint, with an increased incidence of arthritis as the size of the ulnar facet increases.[23]

Nakamura et al. reported that the shortest distance between the capitate and triquetrum (the C-T distance), measured on plain AP radiographs or coronal CT, was the best determinant of lunate type, and that the C-T distance increased as the actual width of the ulnar facet increased.[33] Nakamura et al. defined type I lunates as having a C-T distance of <2 mm and type II lunates as having a C-T distance of >4 mm.[20] In this study, the average C-T distance of type I lunates was 2.50 mm (R, 0.70–3.65; SD, 1.05), which was higher than that reported by Nakamura et al.[33] Lunates with small, cartilaginous ulnar facets had an average C-T distance of 2.68 mm (R, 2.20–3.18; SD, 0.49). This suggests that C-T distance measured on plain AP radiographs cannot discriminate between type I lunates and type II lunates with small cartilaginous facets, and radiographs could therefore not be used routinely to differentiate lunate types. Galley et al. recognized this, defining a third, intermediate group (2.1 mm $<$ C-T distance $<$ 4.0 mm) that included a mixture of type I and type II lunates.[21] Other authors recognized the difficulty in differentiating lunate types with small cartilaginous facets, instead choosing to define a type II lunate as having a distinct ulnar facet of at least 10% of the articular surface.[37] Subsequently, this definition included those lunates with small, cartilaginous facets in the type I lunate group.[37]

The authors found no clear definition of a type II lunate in the literature. The absence of a clear definition of a type II lunate has led to inconsistencies in the reporting of lunate type, with some studies including lunates with a small ulnar cartilaginous facet in a type I group,[33,37,40] and others including them in a type II group.[3,12,13,17,23,24,30,36]

The authors believe that lunate type is better described as a spectrum, with type I lunate at 1 end and type II at the other. The authors propose the inclusion of a third group in the definition of lunate type differentiation. Specifically, a third group (type III) is defined by a small cartilaginous ulnar facet, and lies between type I and type II lunates in this spectrum (Table 1). This group cannot be accurately differentiated by plain AP radiographs or coronal CT. Differentiation of this type requires MRI,[25,37] combined with direct visualization at arthroscopy[41] or dissection.[12,13,24] If differentiation of this third type is clinically irrelevant or not required, then plain AP radiographs and coronal CT can be used to dichotomize lunate type. However, investigators should be aware that these techniques will lead to lunates with small cartilaginous ulnar facets being included in both groups, which may lead to an inconsistency of results and make comparisons with previous literature difficult. Further research is required to examine the differences between type I and II lunates and lunates with a small ulnar cartilaginous facet (type III).

Hamate

Several investigators have observed differences in the shape of the hamate articular surface at the TqH joint.[6,14,42–45] However, a categorization of the hamate has only recently been reported.[26] Consequently, no literature exists comparing hamate type with variations in ligament composition and distribution, differences in carpal kinematics and pathomechanics, different techniques for imaging interpretation, or variations in surgical outcomes. The incidence of type II hamates reported in this study (53%) was lower than that reported by McLean et al. (67%).[26] Considerable cartilage erosion with exposed chondral bone was evident at dissection in 14% of the type I hamates and 50% of the type II (31% overall), which was consistent with other studies of the TqH joint (28%).[17]

The morphology of the hamate at the TqH joint was difficult to categorize. Unlike the other morphological parameters investigated in this study, the hamate groove and distal ridge were not always easily visualized at dissection. In most dissected specimens, the distal ridge had a varying amount of soft tissue attached to it, which made differentiating it more difficult. In most cases, 3-dimensional CT provided the best method of visualization of the hamate joint surface and the distal ridge.

Using mathematical disarticulation of the triquetrum from the hamate, the surface of the hamate could be moved in 3 dimensions and viewed in any plane, and the presence or absence of the distal ridge could be thoroughly examined (Figs. 3, 4). However one (1/13) of the cadaveric specimens produced a poor 3-dimensional reconstruction, with the bony algorithm failing to differentiate severe, widespread chondrocalcinosis from the osseous elements being investigated. This made mathematical disarticulation of the triquetrum from the hamate difficult, despite meticulous bone remodeling. Further research is required to examine the differences between hamate types, any differences in carpal kinematics and pathomechanics, and variations in surgical outcomes.

Capitate

Several investigators have observed differences in the shape of the capitate head.[6,20,25,46] A categorization of the different shapes of the capitate head has only recently been proposed.[27] Consequently, no literature exists comparing capitate type with variations in ligament composition and distribution, differences in carpal kinematics and pathomechanics, or variations in surgical outcomes. The incidence of capitate type reported in this study was 8% V-type, 38% F-type and 54% S-type, which was at variance to that reported by Yazaki et al. (14%, 64.5%, and 21.5%, respectively).[27]

Capitate type could not be routinely identified by plain AP radiographs, which was consistent with the findings of Yazaki et al.[27] Coronal CT and MRI imaging could accurately differentiate F type from the other types, but could not routinely differentiate S-type and V-type capitates. Accurate interpretation of capitate type required extensive dissection. The authors postulate that CT imaging or MRI in the axial plane, perpendicular to that of scapholunate articulation, might provide a more accurate means of differentiating capitate type compared to the standard coronal plane used in this study. Further research is required to examine the differences between capitate types, any differences in carpal kinematics and pathomechanics, and variations in surgical outcomes (especially that of proximal row carpectomy).

REFERENCES

1. Garcia-Elias M, Cooney WP III, An K, Linscheid RL, Chao WYS. Wrist kinematics after limited intercarpal arthrodesis. J Hand Surg 1989;14A:791–799.
2. Berger RA. The anatomy of the ligaments of the wrist and distal radioulnar joints. Clin Orthop Relat Res 2001;383:32–40.
3. Viegas SF. Variations in the skeletal morphologic features of the wrist. Clin Orthop Relat Res 2001;383:21–31.
4. Taleisnik J. The wrist. New York: Churchill Livingstone, 1985:340–442.
5. Moritomo H, Viegas SF, Nakamura K, Dasilva MF, Patterson RM. The scaphotrapezio-trapezoidal joint. Part 1: an anatomic and radiographic study. J Hand Surg 2000;25A:899–910.
6. Kauer JM. The mechanism of the carpal joint. Clin Orthop Relat Res 1986;202:16–26.
7. Compson JP, Waterman JK, Heatley FW. The radiological anatomy of the scaphoid. Part 1: osteology. J Hand Surg 1994;19B:183–187.
8. Nuttall D, Trail IA, Stanley JK. Movement of the scaphoid in the normal wrist. J Hand Surg 1998;23B:762–764.
9. Berger RA. The ligaments of the wrist. A current overview of anatomy with considerations of their potential functions. Hand Clin 1997;13:63–82.
10. Moritomo H, Viegas SF, Elder K, Nakamura K, Dasilva MF, Patterson RM. The scaphotrapezio-trapezoidal joint. Part 2: a kinematic study. J Hand Surg 2000;25A:911–920.
11. Rouvière H. Anatomie humaine, descriptive et topographiqie [Human descriptive anatomy and topography]. Vol. 1. Paris: Masson & Cie, 1924:7–79.
12. Viegas SF, Wagner K, Patterson R, Peterson P. Medial (hamate) facet of the lunate. J Hand Surg 1990;15A:564–571.
13. Viegas SF. The lunatohamate articulation of the midcarpal joint. Arthroscopy 1990;6:5–10.
14. Burgess RC. Anatomic variations of the midcarpal joint. J Hand Surg 1990;15A:129–131.
15. Testut L. Traité d'anatomie humaine [Human anatomy addressed.]. 8th ed. Latarjet A, ed. Vol. I. Paris: Doin, 1930:Testut1188.
16. Antuña-Zapico JM. Disease of the lunate (PhD thesis). Valladolid, Spain: Universidad de Valladolid, 1966:1–100.
17. Viegas SF, Patterson RM, Hokanson JA, Davis J. Wrist anatomy: incidence, distribution, and correlation of anatomic variations, tears, and arthrosis. J Hand Surg 1993;18A:463–475.
18. Viegas SF, Patterson RM, Todd PD, McCarty P. Load mechanics of the midcarpal joint. J Hand Surg 1993;18A:14–18.
19. Viegas SF. Advances in the skeletal anatomy of the wrist. Hand Clin 2001;17:1–11, v.
20. Nakamura K, Beppu M, Patterson RM, Hanson CA, Hume PJ, Viegas SF. Motion analysis in two dimensions of radial-ulnar deviation of type I versus type II lunates. J Hand Surg 2000;25A:877–888.
21. Galley I, Bain GI, McLean JM. Influence of lunate type on scaphoid kinematics. J Hand Surg 2007;32A:842–847.
22. Haase SC, Shin AY, Berger RA. Association between lunate morphology and carpal collapse patterns in scaphoid nonunions. J Hand Surg 2007;32A:1009–1012.
23. Nakamura K, Patterson RM, Moritomo H, Viegas SF. Type I versus type II lunates: ligament anatomy and presence of arthrosis. J Hand Surg 2001;26A:428–436.
24. Sagerman SD, Hauck RM, Palmer AK. Lunate morphology: can it be predicted with routine x-ray films? J Hand Surg 1995;20A:38–41.
25. Pfirrmann CW, Theumann NH, Chung CB, Trudell DJ, Resnick D. The hamatolunate facet: characterization and association with cartilage lesions—magnetic resonance arthrography and anatomic correlation in cadaveric wrists. Skeletal Radiol 2002;31:451–456.
26. McLean J, Bain G, Eames M, Fogg Q, Pourgiezis N. An anatomic study of the triquetrum-hamate joint. J Hand Surg 2006;31A:601–607.
27. Yazaki N, Burns ST, Morris RP, Andersen CR, Patterson RM, Viegas SF. Variations of capitate morphology in the wrist. J Hand Surg 2008;33A:660–666.
28. Kauer JM. The mechanism of the carpal joint. Clin Orthop Relat Res 1986;202:16–26.
29. Garcia-Elias M. Anatomy of the wrist. In: Watson H, Weinzweig J, eds. The wrist. Philadelphia. Lippincott Williams and Wilkins, 2001:7–20.

30. Dyankova S. Anthropometric characteristics of wrists joint surfaces depending on lunate types. Surg Radiol Anat 2007;29:551–559.
31. Fogg QA. Scaphoid variation and an anatomical basis for variable carpal mechanics [thesis]. Adelaide, Australia: University of Adelaide; 2004:161–221.
32. Landis JR, Koch GG. The measurement of observer agreement for categorical data. Biometrics 1977;33:159–174.
33. Nakamura K, Beppu M, Matushita K, Arai T, Ide T. Biomechanical analysis of the stress force on midcarpal joint in Kienböck's disease. Hand Surg 1997;2:101–115.
34. Bland JM, Altman DG. Measuring agreement in method comparison studies. Stat Methods Med Res 1999;8:135–160.
35. Altman DG, Bland JM. Diagnostic tests. 1: sensitivity and specificity. BMJ 1994;308:1552.
36. Haase SC, Berger RA, Shin AY. Association between lunate morphology and carpal collapse patterns in scaphoid nonunions. J Hand Surg 2007;32A:1009–1012.
37. Malik AM, Schweitzer ME, Culp RW, Osterman LA, Manton G. MR imaging of the type II lunate bone: frequency, extent, and associated findings. Am J Roentgenol 1999;173:335–338.
38. Sagerman SD, Zogby RG, Palmer AK, Werner FW, Fortino MD. Relative articular inclination of the distal radioulnar joint: a radiographic study. J Hand Surg 1995;20A:597–601.
39. Patterson RM, Viegas SF, Elder K, Buford WL. Quantification of anatomic, geometric, and load transfer characteristics of the wrist joint. Semin Arthroplasty 1995;6:13–19.
40. Dharap AS, Al-Hashimi H, Kassab S, Abu-Hijleh MF. The hamate facet of the lunate: a radiographic study in an Arab population from Bahrain. Surg Radiol Anat 2006;28:185–188.
41. Viegas SF. Midcarpal arthroscopy: anatomy and portals. Hand Clin 1994;10:577–587.
42. McConaill MA. The mechanical anatomy of the carpus and its bearing on some surgical problems. J Anat 1941;75:166–175.
43. Moritomo H, Goto A, Sato Y, Sugamoto K, Murase T, Yoshikawa H. The triquetrum-hamate joint: an anatomic and in vivo three-dimensional kinematic study. J Hand Surg 2003;28A:797–805.
44. Johnson H. Varying positions of the carpal bones in the different movements at the wrist. J Anat Phys 1907;41:109–122.
45. Weber ER. Concepts governing the rotational shift of the intercalated segment of the carpus. Orthop Clin North Am 1984; 15:193–207.
46. Peh WC, Gilula LA. Normal disruption of carpal arcs. J Hand Surg 1996;21A:561–566.

APPENDIX 3

An association between lunate morphology and scaphoid-trapezium-trapezoid arthritis

J Hand Surg Eur Vol OnlineFirst, published on September 28, 2009 as doi:10.1177/1753193409345201

JHS(E)

The Journal of Hand Surgery (2009) 0: 0: 1–5

AN ASSOCIATION BETWEEN LUNATE MORPHOLOGY AND SCAPHOID–TRAPEZIUM–TRAPEZOID ARTHRITIS

J. M. MCLEAN, P. C. TURNER, G. I. BAIN, N. REZAIAN, J. FIELD and Q. FOGG

From the Discipline of Orthopaedics and Trauma, The University of Adelaide, Adelaide Dept of Orthopaedic Surgery, Modbury Public Hospital, Modbury, Dept of Radiology, Royal Adelaide Hospital and Faculty of Health Sciences, University of Adelaide, Adelaide, South Australia, Australia

The purpose of this study was to determine if an association exists between scaphoid–trapezium–trapezoid arthritis and lunate morphology. Plain neutral posteroanterior radiographs were evaluated for 48 patients with STT arthritis and 96 patients from a control group. Lunate type was determined using capitate–triquetrum (C-T) distance. A type I lunate was defined as a C-T distance $\leq$2 mm. A type II lunate was defined as a C-T distance $\geq$4 mm. Lunate type was recorded and compared between those with STT arthritis and a control group. The groups were similar with regard to age, gender and handedness. Type II lunates were found in 83% of cases with STT arthritis and in 64% of controls. STT OA was associated with type II lunate wrists ($P = 0.02$; OR = 0.35; CI: 0.15–0.82). We postulate that variations in scaphoid motion secondary to lunate morphology may contribute to the development of STT OA.

Keywords: scaphoid–trapezium–trapezoid, STT, arthritis, lunate, morphology

INTRODUCTION

Scaphoid–trapezium–trapezoid (STT) osteoarthritis (OA) affects 6–16% of women in their fifth to seventh decades (Hastings, 2005). Some researchers have postulated that arthritic erosion of the STT joint loosens the constraints of the STT articulation, resulting in instability at the STT joint (Ferris et al., 1994). Others have put forward loss of articular congruity (Meier et al., 2003) or instability of the STT joint (Pinto et al., 2003) as causes of STT OA. These hypotheses suggest that whether STT OA is a cause of, or the consequence of, instability of the STT joint, alterations in the normal kinematics of the STT joint are associated with STT OA.

Viegas et al. (1990) classified two types of lunate based on the midcarpal distal articulation of the lunate. A type I lunate has a single distal facet for the capitate, and does not articulate with the hamate (Fig 1a). A type II lunate has two distal facets; the radial facet articulates with the capitate and the ulnar facet articulates with the hamate (Fig 1b). Type I and II lunates can be differentiated on plain radiographs by the presence or absence of this hamate facet (Viegas et al., 1990). Variations in the morphology of the lunate are associated with variations in wrist kinematics (Galley et al., 2007; Nakamura et al., 2000) and pathomechanics (Haase et al., 2007), ligament composition and distribution (Viegas, 2001), and various carpal pathologies (Nakamura et al., 2001; Viegas, 2001). Midcarpal OA at the lunate–hamate joint was largely confined to type II lunate wrists, suggesting that wrist morphology was a determinant in the development of midcarpal OA (Viegas et al., 1993). Several investigators have suggested that variations in morphology contribute to differences in carpal kinetics, joint loading and soft tissue constraints, which influence the patterns of OA seen at the wrist (Haase et al., 2007; Nakamura et al., 2001; Viegas, 2001).

The shape of the lunate influences the movement of the scaphoid during ulnar and radial deviation (Galley et al., 2007; Moritomo et al., 2000). As motion at the STT joint is closely related to scaphoid kinematics, it is possible that variations in lunate morphology may be related to the pathogenesis of STT OA.

The purpose of this study was to determine if an association exists between lunate morphology and midcarpal STT arthritis.

METHODS

After obtaining ethical approval, a retrospective patient record and radiographic review was performed. Forty-eight patients with the diagnosis of STT arthritis seen at the Royal Adelaide Hospital between January 2000 and January 2007 were identified using a customized database search of plain radiographic reports. Posteroanterior (PA) and lateral wrist radiographs were examined. Only radiographs showing adequate distal radioulnar overlap and a radius-third metacarpal angle of less than 20° from neutral (Yang et al., 1997) were accepted. When several series of plain wrist radiographs were available, the earliest films that demonstrated STT arthritis were used. Radiographs were

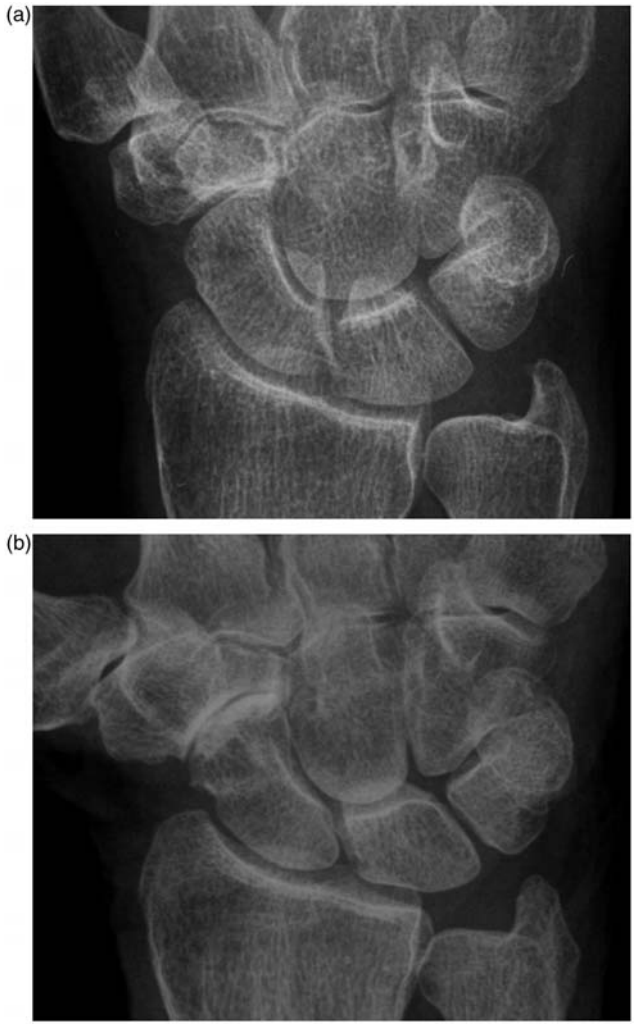

Fig 1 Posteroanterior (PA) radiographs of right wrists demonstrating a type I lunate (a) with a single midcarpal articulating facet with the capitate, and a type II lunate (b) with two midcarpal articulating facets, one with the capitate and the other with the hamate. (b) also demonstrates STT arthritis.

analysed using a Samsung digital viewer with IMPAX 6.0 software (IMPAX, Agfa HealthCare NV, Mortsel, Belgium).

Patients with Grade 2–4 degenerative changes were included in the STT OA group (Eaton and Glickel, 1987). Exclusion criteria included inadequate alignment of radiographs, previous wrist surgery or injury, congenital abnormalities of the wrist and inflammatory arthritis. Patients with radiological parameters suggesting scapholunate dissociation (SLD) or dorsal intercalated segment instability (DISI) were excluded, as these conditions may be associated with STT OA (Crosby et al., 1978; Gilula, 1995). A DISI deformity was defined as a radiolunate angle of greater than -15° on a true lateral wrist radiograph (Linscheid, 1986; Nakamura et al., 1989). A SLD deformity was defined as a scapholunate angle greater than 80° on a true lateral wrist radiograph (Garcia-Elias and Geissler, 2005).

Ninety-six patients over the age of 50 years were selected from the same database as a control group by searching for wrist radiographs taken between 2000 and 2007, on patients who presented to the outpatient or emergency department with pain or acute trauma to the hand. This search produced several pages of potential control patients in alphabetical name order. Five patients from each page were selected; radiographs were not viewed until the selection was complete. No patients with STT OA were included in the control group. Patients with a fracture or dislocation of any carpal bone, history of previous wrist surgery or injury, congenital abnormalities of the wrist and inflammatory arthritis were excluded.

In the STT OA group, there were 18 male and 30 female patients. The average age was 76 years (range: 50–96); 21 were left and 27 were right wrists. The control group comprised 45 male and 51 female patients. The average age was 73 years (range: 50–100); 46 were left and 50 were right wrists.

For each radiograph, the lunate was classified as type I or type II (Viegas et al., 1990) (Fig 1). We identified type I and type II lunate wrists from the neutral PA radiograph using the shortest distance between the capitate and triquetrum (C-T distance), which increases as the width of the medial lunate facet increases (Nakamura et al., 1997). The type I lunate group was defined as a C-T distance ≤ 2 mm and type II lunate group was defined as a C-T distance ≥ 4 mm. A third intermediate group (2.1 mm $\leq$ C-T distance $\leq$ 4.0 mm) was excluded from the study, to minimize the possibility of including some type II lunates with a small medial facet in a type I group.

Two independent observers each inspected every radiograph on two occasions. Where there was disagreement between observers, the mode was used to assign lunate type. C-T distance inter-observer agreement was assessed using the method of Altman and Bland (1994). Intra- and inter-observer kappa statistics were performed to assess agreement using the method of Landis and Koch (1977).

Standard t tests, Fisher's exact test and linear regression methods were used to analyse the data. Statistical significance was set at $P < 0.05$.

RESULTS

There was no significant difference between the two groups for age ($P = 0.07$), gender ($P = 0.373$) or handedness ($P = 0.724$), and there was no significant difference between genders in the distribution of type I and type II lunates ($P = 0.715$).

The average inter-observer difference for C-T distance was 0.05. The kappa value for inter-observer variability was 0.96. Kappa value for intra-observer variability was 0.95.

In the STT OA group, there were eight type I lunate wrists and 40 type II lunate wrists. In the control group, there were 35 type I lunate wrists and 61 type II lunate wrists. Type II lunate wrists were strongly associated with STT osteoarthritis ($P = 0.02$; OR $= 0.35$; 95% CI: 0.15–0.82).

DISCUSSION

This study demonstrated an association between STT OA and type II lunate wrists. The proportion of type II lunates in the control group (64%) was similar to previous studies (63% to 73%) (Burgess, 1990; McLean et al., 2009; Viegas, 1990; Viegas et al., 1990; 1993).

Nakamura et al. (1997) reported that the shortest distance between the capitate and triquetrum (C-T distance) on a plain PA radiograph increased as the width of the medial facet increased. We also identified type I and type II lunate wrists using C-T distance measured on neutral PA radiograph, to minimize the possibility of including some type II lunates with a small medial facet in a type I group.

Galley et al. (2007) demonstrated that wrists with different lunate morphology have significantly different kinematics during radial–ulnar deviation of the wrist. Wrists with a type I lunate show greater scaphoid translation, while wrists with a type II lunate show greater scaphoid flexion.

It has been hypothesized that the midcarpal articulation of a wrist with a type II lunate works in the same way as a 'knee joint', restricting the amount of rotation and translation of the joint, and forcing it to work in a flexion–extension plane (Fig 2) (Galley et al., 2007; Watts et al., 2009). In contrast, motion at the midcarpal joint of a wrist with a type I lunate is not restricting to the predominant flexion–extension plane like a type II lunate wrist (Watts et al., 2009). A type I lunate wrist allows rotation and translation between the proximal and distal carpal rows (Fig 3).

In this concept, there are two distinct types of scaphoid, with a spectrum of variation in-between (Ceri et al., 2004; Watts et al., 2009). Differences in the ligament attachments of the two scaphoid types suggest that during wrist motion, one type of scaphoid primarily rotates about its longitudinal axis, while the other type primarily flexes–extends about its longitudinal axis (Watts et al., 2009).

The ligamentous complex that guides the predominant flexion–extension motion of a scaphoid associated with a type II lunate is different from that associated with a type I lunate (Nakamura et al., 2001; Viegas, 2001; Viegas et al., 1993; Watts et al., 2009). We hypothesize that a ligament complex that guides a wrist with a type II lunate is more rigid, allowing predominantly flexion–extension motion at the midcarpal joint and at the STT joint. In this concept, any change to the normally rigid flexion–extension kinematics of a type II lunate wrist may

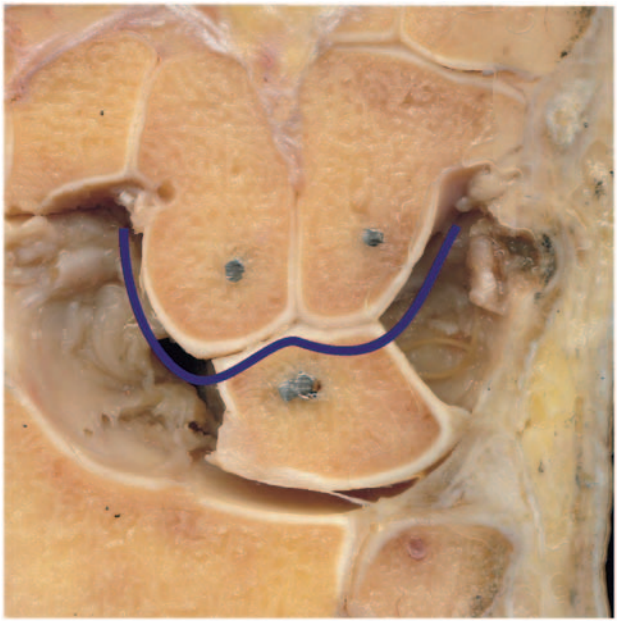

Fig 2 The midcarpal articulation of a wrist with a type II lunate (indicated by the blue line) in a cadaveric coronal section of a right wrist. The midcarpal joint may restrict rotation and translation, forcing the midcarpal joint to work in a flexion–extension plane.

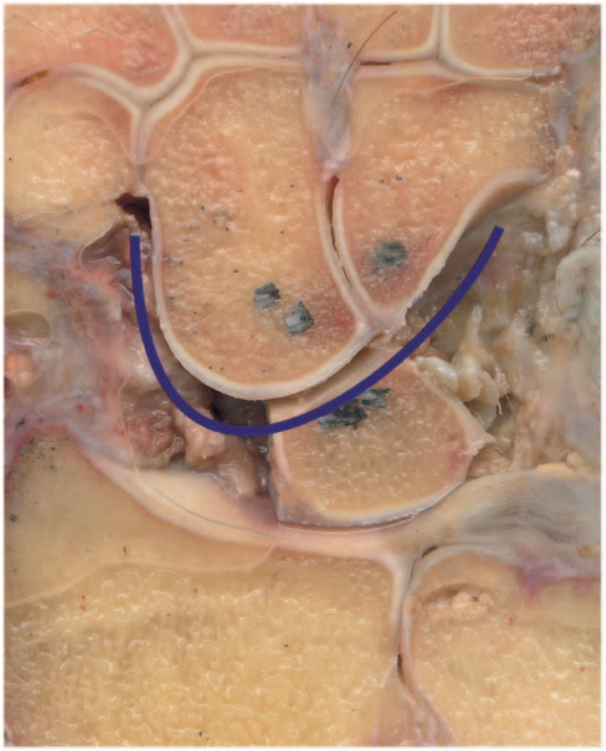

Fig 3 The midcarpal articulation of a wrist with a type I lunate (indicated by the blue line). The configuration of the midcarpal joint allows rotation and translation between the proximal and distal carpal rows.

potentiate conditions suitable for the development of arthrosis at the STT and midcarpal joints. By this mechanism, we postulate that lunate morphology is associated with variations in scaphoid motion, and that these differences may contribute to the development of STT OA in type II lunate wrists.

We acknowledge limitations of this radiographic study. We chose to use plain PA radiographs to differentiate lunate types according to the method of Nakamura et al. (1997). Plain radiographs have been used extensively in the literature, and represent the most common and most widely accepted method of dichotomizing lunate type according to the classification of Viegas et al. (1990). In a study comparing radiographic techniques, plain radiographs have been reported to have similar accuracy in determining lunate type when compared to computed tomography (McLean et al., 2009). The kappa values reported in this study reflect low inter- and intra-observer variability using this method of lunate classification, which was comparable to previous studies (McLean et al., 2009; Sagerman et al., 1995).

A type II lunate wrist, in which there is a large lunohamate facet, can be routinely identified radiographically when compared with a type I lunate (Sagerman et al., 1995). However, very small cartilaginous ulnar facets are not always identifiable on plain radiographs or coronal CT (McLean et al., 2009; Nakamura et al., 1997; Sagerman et al., 1995). As this investigation determined lunate type based on two-dimensional radiographs it is possible that some lunates with very small cartilaginous ulnar facets may have been included in the type II lunate group. We attempted to minimize the possibility of including some type II lunates with a small medial facet in a type I group, by using C-T distance to assign lunate type. This led to intermediate lunate wrists being excluded from the study, and ensured a more accurate comparison between type I and II lunate wrists. Further research is required to investigate the relationship between midcarpal morphology and carpal kinematics.

CONFLICT OF INTERESTS

Financial support was received from the Royal Australasian College of Surgeons (RACS), including a RACS Foundation W. G. Norman Research Scholarship, and from the Modbury Public Hospital Foundation, including a research grant, for Dr. James M. McLean while he undertook a Masters of Surgery at the University of Adelaide, Adelaide, South Australia, Australia.

Acknowledgements

Royal Australasian College of Surgeons Foundation for support through W. G. Norman Research Fellowship. Modbury Public Hospital Foundation for support through a Research Grant. Mr Ian Galley MBChB for guidance in establishing the research goals.

References

Altman DG, Bland JM. Diagnostic tests. 1: Sensitivity and specificity. BMJ. 1994, 308: 1552.

Burgess RC. Anatomic variations of the midcarpal joint. J Hand Surg Am. 1990, 15: 129–31.

Ceri N, Korman E, Gunal I, Tetik S. The morphological and morphometric features of the scaphoid. J Hand Surg Br. 2004, 29: 393–8.

Crosby EB, Linscheid RL, Dobyns JH. Scaphotrapezial trapezoidal arthrosis. J Hand Surg Am. 1978, 3: 223–34.

Eaton RG, Glickel SZ. Trapeziometacarpal osteoarthritis. Staging as a rationale for treatment. Hand Clin. 1987, 3: 455–71.

Ferris BD, Dunnett W, Lavelle JR. An association between scapho-trapezio-trapezoid osteoarthritis and static dorsal intercalated segment instability. J Hand Surg Br. 1994, 19: 338–9.

Galley I, Bain GI, McLean JM. Influence of lunate type on scaphoid kinematics. J Hand Surg Am. 2007, 32: 842–7.

Garcia-Elias M, Geissler WB. Carpal instability. In: Green DP et al. (Eds.) *Green's Operative Hand Surgery*, 5th Edn. Philadelphia, Churchill Livingstone, 2005: 535–604.

Gilula LA. Dorsal intercalated segment instability (DISI) and scapho-trapezio-trapezoid (STT) osteoarthritis. J Hand Surg Br. 1995, 20: 264.

Haase SC, Berger RA, Shin AY. Association between lunate morphology and carpal collapse patterns in scaphoid nonunions. J Hand Surg Am. 2007, 32: 1009–12.

Hastings H. Arthrodesis. In: Green DP et al. (Eds.) *Green's Operative Hand Surgery*, 5th Edn. Philadelphia, Churchill Livingstone, 2005: 489–534.

Landis JR, Koch GG. The measurement of observer agreement for categorical data. Biometrics. 1977, 33: 159–74.

Linscheid RL. Kinematic considerations of the wrist. Clin Orthop Relat Res. 1986, 202: 27–39.

McLean JM, Bain GI, Watts AC, Mooney LT, Turner PC, Moss M. Imaging recognition of morphological variants at the midcarpal joint. J Hand Surg Am. 2009, 34: 1044–55.

Meier R, Prommersberger KJ, Krimmer H. [Scapho-trapezio-trapezoid arthrodesis (triscaphe arthrodesis).]. Handchir Mikrochir Plast Chir. 2003, 35: 323–7.

Moritomo H, Viegas SF, Elder KW et al.. Scaphoid nonunions: a 3-dimensional analysis of patterns of deformity. J Hand Surg Am. 2000, 25: 520–8.

Nakamura K, Beppu M, Matushita K, Arai T, Ide T. Biomechanical analysis of the stress force on midcarpal joint in Kienbock's disease. Hand Surg. 1997, 2: 101–15.

Nakamura K, Beppu M, Patterson RM, Hanson CA, Hume PJ, Viegas SF. Motion analysis in two dimensions of radial–ulnar deviation of type I versus type II lunates. J Hand Surg Am. 2000, 25: 877–88.

Nakamura R, Hori M, Imamura T, Horii E, Miura T. Method for measurement and evaluation of carpal bone angles. J Hand Surg Am. 1989, 14: 412–16.

Nakamura K, Patterson RM, Moritomo H, Viegas SF. Type I versus type II lunates: Ligament anatomy and presence of arthrosis. J Hand Surg Am. 2001, 26: 428–36.

Pinto CH, Obermann WR, Deijkers RL. Nontraumatic multidirectional instability of the scaphotrapeziotrapezoid joint: a cause of scaphotrapeziotrapezoid osteoarthritis and static distal intercalated segment instability. J Hand Surg Am. 2003, 28: 744–50.

Sagerman SD, Hauck RM, Palmer AK. Lunate morphology: can it be predicted with routine x-ray films? J Hand Surg Am. 1995, 20: 38–41.

Viegas SF. The lunatohamate articulation of the midcarpal joint. Arthroscopy. 1990, 6: 5–10.

Viegas SF. Variations in the skeletal morphologic features of the wrist. Clin Orthop Relat Res. 2001, 383: 21–31.

Viegas SF, Patterson RM, Hokanson JA, Davis J. Wrist anatomy: incidence, distribution, and correlation of anatomic variations, tears, and arthrosis. J Hand Surg Am. 1993, 18: 463–75.

Viegas SF, Wagner K, Patterson R, Peterson P. Medial (hamate) facet of the lunate. J Hand Surg Am. 1990, 15: 564–71.

Watts AC, McLean JM, Fogg Q, Bain GI. Scaphoid anatomy. In: Slutsky DJ, Slade JF (Eds.) *The scaphoid*. New York, Thieme Medical Publishers, 2009: in press.

Yang Z, Mann FA, Gilula LA, Haerr C, Larsen CF. Scaphopisocapitate alignment: criterion to establish a neutral lateral view of the wrist. Radiology. 1997, 205: 865–69.

Received: 23 March 2009
Revised: 28 June 2009
Accepted after revision: 17 July 2009
Mr Gregory I. Bain, 196 Melbourne St, North Adelaide SA, 5006, Australia.
Tel.: +61 8 8361 8399; fax: +61 8 8239 2237.
E-mail: greg@gregbain.com.au.

doi: 10.1177/1753193409345201 available online at http://jhs.sagepub.com

APPENDIX 4

Translunate fracture with associated perilunate injury: 3 case reports with introduction of the translunate arc concept

Translunate Fracture With Associated Perilunate Injury: 3 Case Reports With Introduction of the Translunate Arc Concept

Gregory I. Bain, PhD, James M. McLean, MBBS, Perry C. Turner, MBChB, Aman Sood, MBBS, Nicholas Pourgiezis, MBBS

We report 3 cases of translunate fractures with associated perilunate dislocations (or subluxation). We believe the translunate injury reflects a higher-velocity trauma and produces further destabilization of the carpus when compared with the established greater and lesser arc injuries. A modification to Johnson's perilunate injury classification system is proposed: the addition of a *translunate arc* injury subgroup, which would include all perilunate injuries with translunate fractures. *(J Hand Surg 2008;33A:1770–1776. Copyright © 2008 by the American Society for Surgery of the Hand. All rights reserved.)*

Key words Greater arc, lesser arc, lunate fracture, perilunate, perilunate dislocation, translunate arc, translunate fracture.

A PERILUNATE FRACTURE-DISLOCATION INVOLVES dislocation of the lunate from the surrounding carpus or the surrounding carpus from the lunate. The mechanism of injury involves a combination of extension, intercarpal supination, and ulnar deviation of the wrist.[1,2] The resulting injury involves progressive stages of failure of intracarpal carpal ligaments from radial to ulna around the lunate as defined by Mayfield[2,3] (Fig. 1). Johnson divided injuries into lesser arc (pure ligamentous) and greater arc (with carpal fracture) injuries.[1] The combined, rare condition of translunate, perilunate fracture-dislocation, is not included in the instability patterns as described by Johnson and Mayfield or in the classification of lunate fractures as described by Teisen and Hjarbaek.[1–4]

From the Department of Orthopaedic and Trauma Surgery, Royal Adelaide Hospital, Adelaide, South Australia, Australia; University of Adelaide, Adelaide, South Australia, Australia; Modbury Public Hospital, Modbury, South Australia, Australia; and The Queen Elizabeth Hospital, Woodville, South Australia, Australia.

The authors would like to acknowledge Ronit Wollstein, MD, Children's Hospital Hand Surgery Center, Pittsburgh, for providing 2 of the cases in this series.

Received for publication February 12, 2008; accepted in revised form June 19, 2008.

No benefits in any form have been received or will be received related directly or indirectly to the subject of this article.

Corresponding author: Gregory I. Bain, PhD, 196 Melbourne St., North Adelaide, SA 5006, Australia; e-mail: greg@gregbain.com.au.

0363-5023/08/33A10-0012$34.00/0
doi:10.1016/j.jhsa.2008.06.017

With a perilunate dislocation, the radiolunate ligaments (long radiolunate ligament and short radiolunate ligament) remain intact, stabilizing the lunate to the radius. When performing a surgical stabilization of a perilunate fracture-dislocation, the surgeon will often stabilize the proximal carpal row to the stable "keystone" lunate. If the lunate is also fractured, this makes the stabilization process considerably more difficult.

To highlight this difficulty, we present 3 cases of translunate fractures with perilunate fracture-dislocation (or subluxation). We suggest the introduction of the term *translunate arc* to the widely used Johnson classification system to emphasize the importance of stabilization of the lunate fracture.[1]

CASE STUDY 1: TRANSLUNATE FRACTURE WITH ASSOCIATED PERILUNATE INJURY (SUBLUXATION AND TRANSCAPITATE FRACTURE)

A 32-year-old electrician fell from a motorcycle at 40 km/h onto an outstretched right hand. He presented to hospital 3 days after the accident with an isolated right wrist injury. Orthopedic examination revealed a diffusely tender, swollen wrist with a palmar skin abrasion and a normal median nerve. Plain radiographs demonstrated a volar fracture of the lunate and an increased angulation between the capitate and lunate with the lunate facing palmarly suggesting a volar intercalated

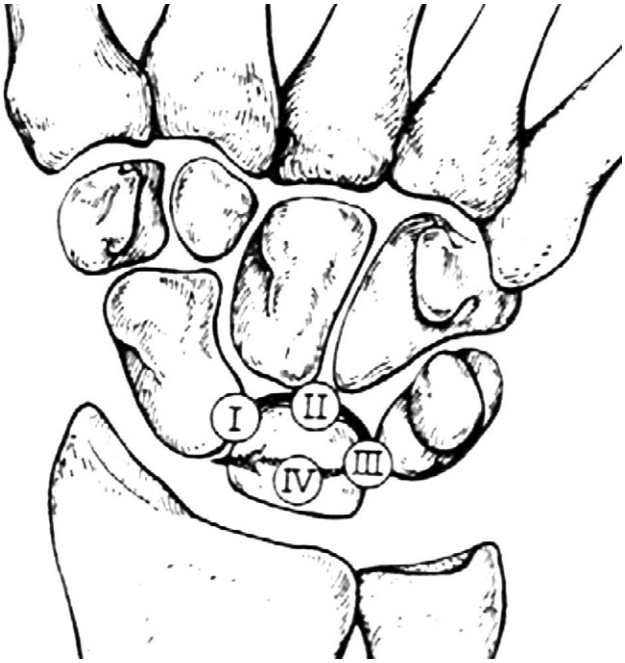

FIGURE 1: Mayfield's 4 stages of perilunate instability. Stage I is disruption of the scapholunate ligament. Stage II is dislocation (usually dorsal) of the capitolunate articulation. Stage III is disruption of the lunotriquetral ligament. Stage IV involves tearing of the dorsal radiocarpal ligaments. (Used with permission. Article published in Orthop Clin North Am, Vol. 15, Mayfield JK. Wrist ligamentous anatomy and pathogenesis of carpal instability. p. 214. Copyright Elsevier 1984.)

segmental instability. Computed tomography (CT) scan of the wrist showed (in addition to the lunate fracture) a transverse capitate fracture and proximal volar subluxation of the capitate head (Fig. 2). The diagnosis of translunate fracture with perilunate injury (transcapitate fracture with perilunate volar subluxation) was made.

Definitive orthopedic surgical treatment occurred 9 days after the initial injury. A volar ulnar approach was used to expose the volar capsule and the carpus, which involved release of the ulna nerve and release of the carpal tunnel.[5] A rent in the volar capsule was identified. A longitudinal incision was made in the volar capsule, and subperiosteal dissection was performed radially and ulnarly to achieve adequate exposure of the carpal bones and fractures. After exposing the lunate and capitate fractures, the osteochondral capitate fracture was reduced and fixed with a Mini-Acutrak cannulated headless screw (Acumed Ltd, Hampshire, UK). The lunate fragment was too small to accommodate a small screw. After obtaining reduction, the lunate fracture fragment was secured using two 1.1-mm (0.043-in) K-wires. The wires were advanced from the volar aspect through the dorsal aspect using a retrograde technique. The closure was performed in layers with meticulous repair of the volar wrist capsule.

After surgery, the wrist was immobilized in a below-elbow volar wrist splint for 6 weeks, with gentle finger range of motion exercises as tolerated. K-wires were removed at 6 weeks and physiotherapy commenced. Radiology follow-up confirmed satisfactory alignment and fixation (Fig. 3A, B). At 4 months, the patient had returned to all his activities of daily living. Examination demonstrated equal wrist flexion and extension of 35°. At 6 months, he continued to complain of pain over the dorsal aspect of his wrist with repetitive forceful grip-release activities while using tools at work. All other activities were pain-free.

CASE STUDY 2: TRANSLUNATE FRACTURE WITH PERILUNATE INJURY (DISLOCATION WITH TRANS-STYLOID FRACTURE)

A 37-year-old construction worker fell from a height of 9 m onto a concrete factory floor sustaining multiple severe injuries. Orthopedic injuries included a right wrist translunate fracture with perilunate injury (dislocation and trans-styloid fracture) with dorsal radiolunate subluxation (Fig. 4A). Examination revealed abrasions on the palm and an intact median nerve. The patient received expedient closed operative reduction of the carpus and was transferred to the intensive care unit for hemodynamic stabilization (Fig. 4B). CT scan demonstrated dorsal rotation of the lunate with comminution, widening of the scapholunate interval, and an avulsion fracture of the ulna and radial styloid processes. The patient returned to the operating room 6 days after the initial injury once hemodynamically stable. A dorsal approach through the interspace between the third and fourth compartments was used. A longitudinal incision was made in the dorsal capsule, and subperiosteal dissection was performed radially and ulnarly to achieve adequate exposure of the carpal bones. The lunate was exposed revealing a coronal dorsal lunate fragment. The scapholunate ligament was torn off the lunate. The scaphoid and lunate were reduced and transfixed with two K-wires. The lunate and triquetrum were reduced and fixed with one K-wire (Fig. 5A, B). The scapholunate ligament was repaired to the lunate using two Mini Mitek (3-0 Ethibond; Ethicon, Sommerville, NJ) suture anchors. A layered closure was performed.

After surgery, the wrist was immobilized in a below-elbow volar splint. Orthopedic clinical review was performed at 1, 4, 6, and 8 weeks postoperatively. At 6 weeks, he complained of dorsal wrist pain, and sensation had decreased over the medial nerve distribution. Radiology examination was suggestive of failure of fixation (Fig. 6A,

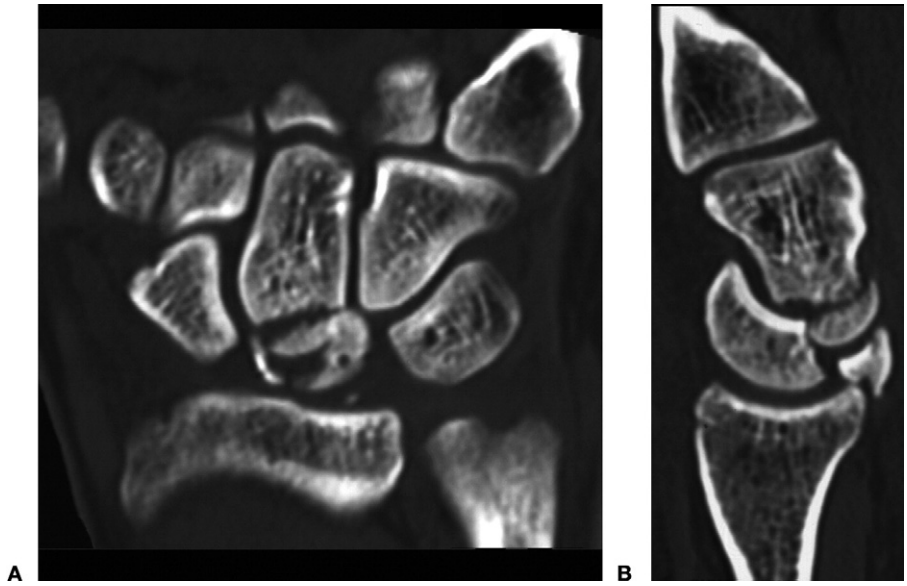

FIGURE 2: Translunate fracture with perilunate injury (subluxation with transcapitate fracture). **A** A coronal CT scan of the right wrist demonstrating a translunate and transcapitate fracture. **B** A sagittal CT scan of the right wrist demonstrating translunate and transcapitate fracture with dislocation of the capitate from the lunate.

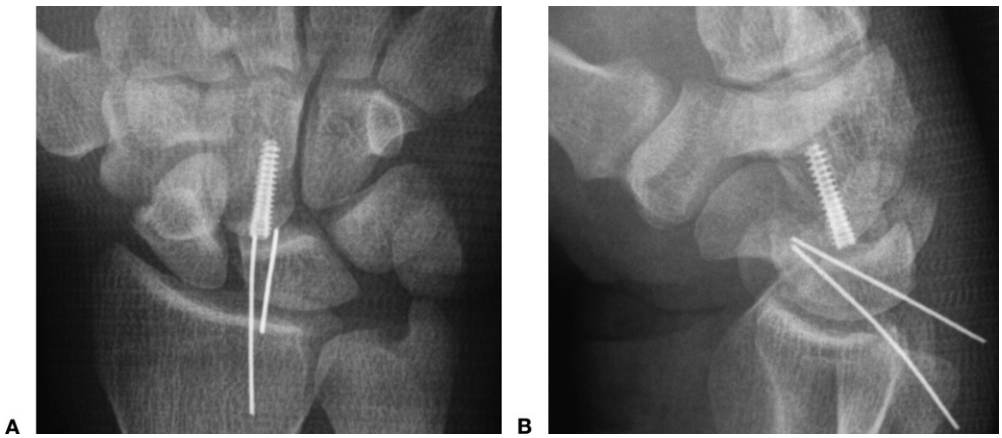

FIGURE 3: Translunate fracture with perilunate injury (subluxation with transcapitate fracture). **A** Posteroanterior radiograph of the right wrist demonstrating reduction of the translunate, transcapitate fracture-dislocation. A cannulated headless screw has been used to fix the capitate, and two 1.1-mm (0.043-in) K-wires have been used to fix the lunate. **B** Lateral radiograph of the right wrist demonstrating reduction of the translunate, transcapitate fracture-dislocation. The normal articular position of the capitate relative to the lunate has been restored.

B). The patient was readmitted for an elective proximal row carpectomy or wrist arthrodesis. Intraoperative inspection of the articulating surface of the distal radius revealed a large degree of chondral loss, therefore the decision was made to perform a wrist arthrodesis.

CASE STUDY 3: TRANSLUNATE FRACTURE WITH PERILUNATE INJURY (DISLOCATION WITH TRANS-SCAPHOID FRACTURE)

A 66-year-old carpenter fell 4.5 m through a mezzanine ceiling onto an outstretched left arm sustaining an isolated left wrist injury. Examination of the left hand and wrist revealed a palmar skin graze, a diffusely tender swollen wrist, and normal median nerve function. Initial plain radiographs demonstrated a volarly displaced and rotated lunate, with an associated fracture of the middle third of the scaphoid, suggestive of a translunate fracture with perilunate injury (dislocation and a trans-scaphoid fracture) (Fig. 7A, B). An unsuccessful attempt at reduction was made. A preoperative CT scan was not performed. The patient

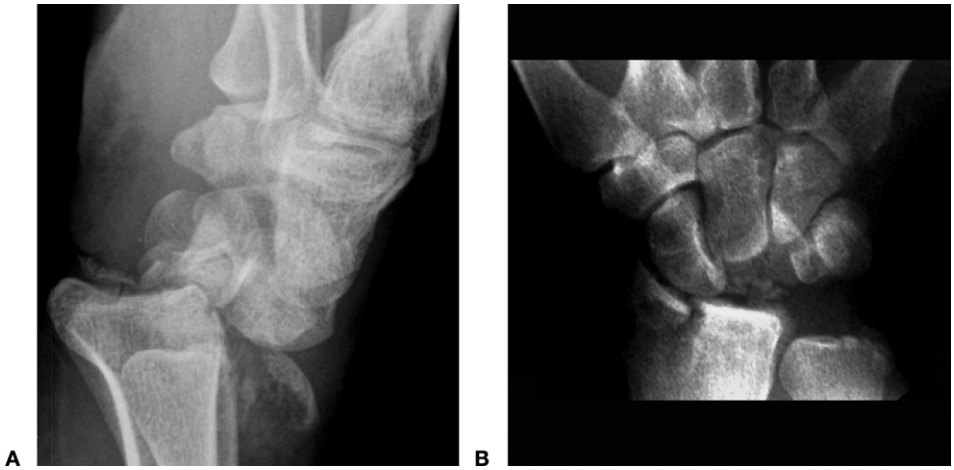

FIGURE 4: Translunate fracture with perilunate injury (dislocation with trans-styloid fracture). **A** A lateral radiograph of the right wrist demonstrating a trans-styloid, translunate, perilunate fracture–dislocation. **B** An intraoperative anteroposterior radiograph of the right wrist. The lunate is dislocated from the capitate head. The trans-styloid fracture has an obvious step-deformity of the radiocarpal articulating surface.

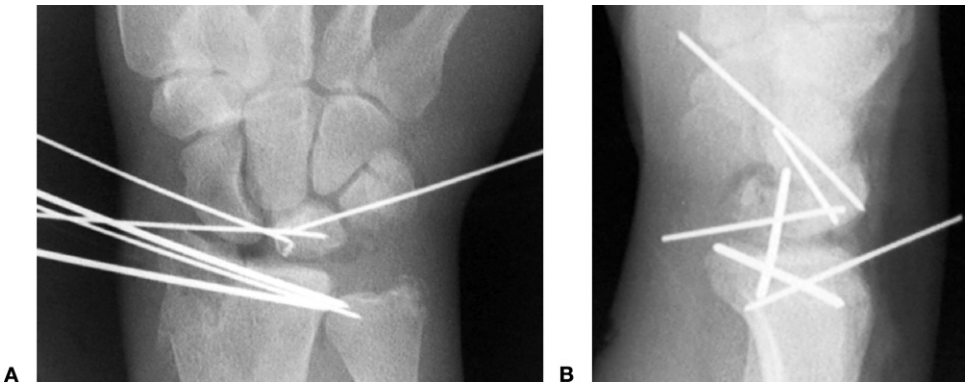

FIGURE 5: Translunate fracture with perilunate injury (dislocation with trans-styloid fracture). **A** An intraoperative posteroanterior radiograph of the right wrist. The translunate and trans-styloid fractures have been reduced and fixed with K-wires. **B** An intraoperative lateral radiograph of the right wrist confirmed a satisfactory reduction and fixation of the translunate, perilunate fracture–dislocation.

proceeded to the operating room the same day for surgical management. A dorsal approach was performed (as previously described). A temporary K-wire was used to hold the scaphoid after reduction of the fracture. Intraoperative clinical examination demonstrated a coronal fracture through the body of the lunate, not appreciated preoperatively. A subsequent volar-ulnar approach was used to expose the lunate, which demonstrated a highly comminuted volar lunate fracture. Attempts to reduce the lunate fragments were unsuccessful secondary to the high degree of comminution. The articulating surface of the proximal capitate and the lunate fossae were intact, and as a consequence, the decision was made to progress to a proximal row carpectomy. The closure was performed in layers with meticulous repair of dorsal and volar wrist capsules.

After surgery, the left wrist was immobilized in a below elbow volar splint for 4 weeks. The patient was reviewed clinically and radiographically at 1 and 4 weeks post-operatively. At 6 weeks, pain had improved considerably, and he began physiotherapy for strength and range of motion exercises. Follow-up is currently to 12 months and he has 25° of wrist flexion and extension with minimal pain.

DISCUSSION

A perilunate fracture-dislocation involves dislocation of the carpus from the lunate with a number of ligamentous and fracture patterns described.[1–3,6] A perilunate injury usually results from high-energy trauma, such as

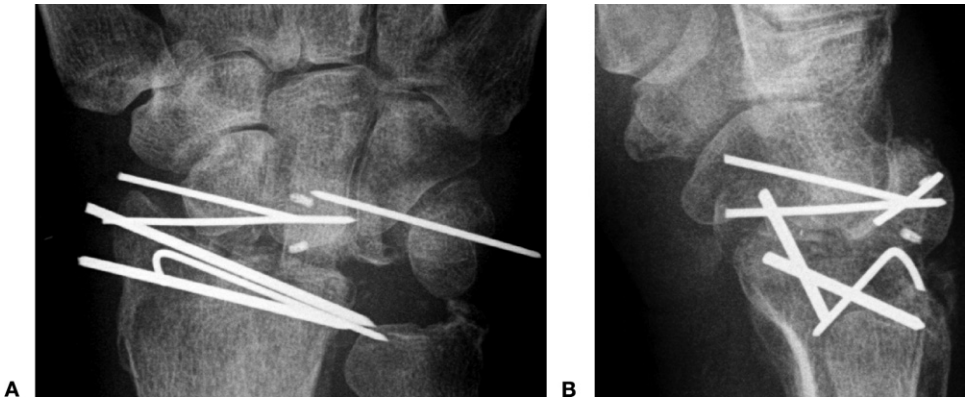

FIGURE 6: Translunate fracture with perilunate injury (dislocation with trans-styloid fracture). **A** Posteroanterior radiograph of the right wrist showing failure of fixation of the volar lunate fragment with dorsal subluxation of the body of the lunate and flexion of the scaphoid and separation of the lunate fragments. **B** Lateral radiograph of the right wrist showing failure of fixation of the volar lunate fragment with dorsal subluxation of the body of the lunate and flexion of the carpus.

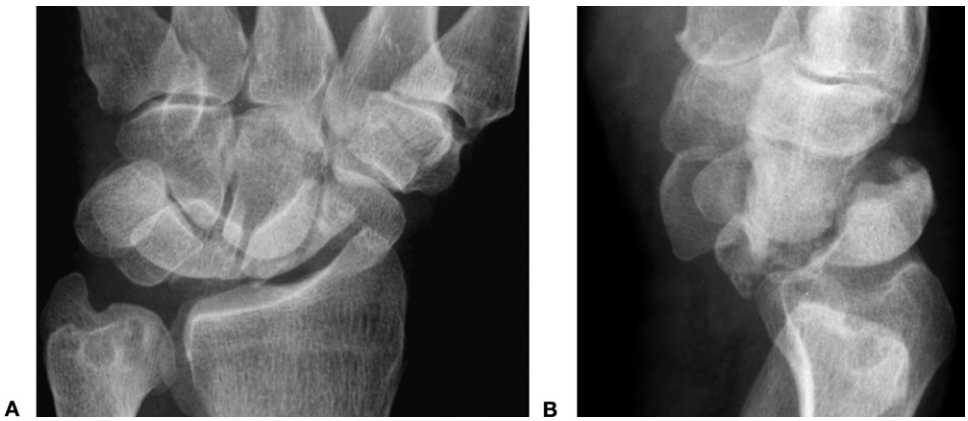

FIGURE 7: Translunate fracture with perilunate injury (dislocation with trans-scaphoid fracture). **A** Posteroanterior radiograph of the left wrist demonstrating a scaphoid and lunate fracture with perilunate dislocation. **B** Lateral radiograph of the left wrist demonstrating a scaphoid and lunate fracture with perilunate dislocation.

a motor vehicle accident or fall from a height.[7] Patients commonly present with wrist pain, swelling, and decreased range of motion. Evidence of median nerve injury is common, and acute carpal tunnel syndrome is present in approximately 25% of patients (range, 16% to 46%).[7–9] Despite the severe disruption of carpal anatomy, perilunate dislocations are often missed in the acute setting, due to the priority of associated life-threatening injuries and a lack of appreciation of complex carpal anatomy by treating emergency physicians and radiologists. In a multicenter study of 166 patients, perilunate injuries were initially missed in 25% of cases.[7]

In a series of cadaveric studies, Mayfield demonstrated that perilunate dislocation was a consequence of progressive ligamentous injury to the carpus that commenced volarly on the radial side, continuing distally around the lunate to the ulnar side of the wrist.[2,3]

The 3 forces involved have been shown to be a combination of wrist extension, intercarpal supination, and ulnar deviation.[1–3] These occur when a force is applied to the palm of an outstretched hand on a fixed pronated radius.[1]

Mayfield classified perilunate dislocation into 4 stages[2,3] (Fig. 1). These involve progressive tearing of carpal ligaments starting with the volar scapholunate ligament (stage I), followed by dislocation (almost always dorsal) of the lunocapitate joint (stage II), and subsequently tearing of the lunotriquetral ligament (stage III). Stage IV involves tearing of the dorsal radiocarpal ligament, allowing the lunate to dislocate volarly, secondary to the unopposed volar radiolunate ligaments (long radiolunate ligament and short radiolunate ligament). The radiolunate ligaments may cause a 180° rotation of the lunate. Mayfield's cadaveric studies were limited to sequential sectioning techniques.[3] As a result, the potential destabiliz-

ing effect that unrestrained ligament attachments have in the presence of a lunate fracture was not included in Mayfield's classification.

Johnson classified perilunate fracture dislocations according to the structures involved.[1] When the immediate surrounding ligaments of the lunate are involved; these are termed *lesser arc* injuries. If a fracture of the carpal bones surrounding the lunate occurs, these are termed *greater arc* injuries. Strictly speaking, only a trans-scaphoid, transcapitate, transtriquetral perilunate dislocation should truly be called a greater arc injury. This modality, however, is extremely unusual, with only 2 cases being reported in the English literature.[10,11] All other perilunate fracture-dislocations combine ligament ruptures, bone avulsions, and fractures in a variety of clinical forms. The most frequent is the dorsal trans-scaphoid perilunate dislocation. Cartilage damage can occur and is most commonly seen on the head of the capitate.[12] Johnson's classification did not include a categorization of lunate fractures or a discussion on the potential destabilizing effects that unrestrained ligament attachments have on various lunate fracture fragments and their relationship to lunate dislocations.

Isolated fractures of the lunate are rare.[4,13–15] Teisen and Hjarbaek divided lunate fractures into 5 groups based on a review of 17 cases collected over a period of 31 years. Their classification system does not incorporate the relationship between lunate fractures, perilunate instability, and lunate dislocations.[4]

Other investigators have discussed similar cases of translunate, perilunate fracture-dislocations (or subluxations) but have made no reference to the classification systems commonly used in the application of treatment principles.[16–20]

The cases discussed involve translunate, perilunate dislocation (or subluxation), with variable combinations of carpal fractures. In all of the cases discussed, the injury pathomechanics are likely to involve a direct, high-energy, volar impact, produced with the wrist hyperextended. The force necessary must be high enough to cause a combined ligament injury and lunate fracture. To the authors' knowledge, this pathomechanical concept has not yet been confirmed by any laboratory investigation. The mechanism of injury in these cases did not fit Mayfield's classification system of perilunate instabilities.[2,3] Indeed, the injuries described are a variable combination of the stages of instability described by Mayfield, with the addition of a translunate fracture. In this situation, a lunate fracture combined with rupture of the scapholunate or lunotriquetral ligaments produces a supplementary destabilizing force, distinct from the translation force exerted by the capitate, typical of a stage IV perilunate dislocation described by Mayfield.[2] The authors recognize that the destabilizing effect secondary to a lunate fracture was not investigated by Mayfield.[2,3] The authors would contend that a lunate fracture should be considered as an independent, supplementary destabilizing force, to be considered when attempting to classify perilunate instabilities.

In translunate fractures, the degree of lunate displacement depends on the destabilizing forces acting on the lunate fracture fragments. The forces influence the fracture pattern, the associated damage to direct supporting ligaments of the lunate, and the associated damage to indirect supporting carpal structures. The long radiolunate and short radiolunate ligaments, the ulnolunate ligament, and the scapholunate and lunotriquetral ligaments may provide substantial destabilizing effects, which should be considered in any translunate fracture. To our knowledge, the combined destabilizing properties of these ligaments have not yet been investigated by any laboratory analysis.

With a perilunate dislocation, the volar radiolunate ligaments remain intact, stabilizing the lunate to the radius. When performing a surgical stabilization of a perilunate fracture-dislocation, the surgeon will often stabilize the proximal carpal row to the stable "keystone" lunate. If the lunate is also fractured, then the treatment algorithm must change—with the surgeon aiming to stabilize the lunate first, and then stabilize the proximal carpal row. The associated lunate fracture makes the stabilization process considerably more difficult.

The authors propose a modification to Johnson's widely accepted classification system of perilunate instabilities[1]; specifically, the addition of a third category of perilunate instability that recognizes the destabilizing forces resulting from, and consequent to, a concurrent lunate fracture. The term *translunate arc* is proposed to include all translunate fractures, with associated perilunate injury (fracture, dislocation, or subluxations) (Fig. 8).

We propose that this term be used in conjunction with the terms *greater arc* and *lesser arc* when classifying perilunate injuries.

The treatment principles involved in the management of translunate arc injuries integrate simplistically with Johnson's original classification system.[12] Specifically, the management principles of a greater arc injury are directed toward reduction and fixation of fractures around the lunate (scaphoid, capitate, and/or triquetrum), followed by the ligamentous repair. The management principles of a lesser arc injury are directed toward repair of the direct stabilizing ligaments of the lunate and include provisional stabilization of the lunate by pinning of the scaphoid and/or triquetrum to the lunate. The management principles of a translunate

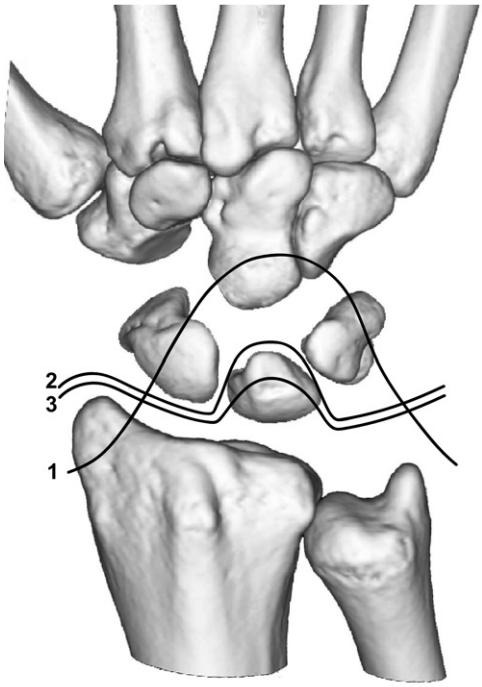

FIGURE 8: Perilunate injury patterns showing greater arc, lesser arc, and translunate arc (Bain's modification to Johnson's original classification system of perilunate injury[1]). Line 1 indicates greater arc injuries, which occur through osseous structures surrounding the lunate, such as the radial styloid, scaphoid, capitate, hamate, and triquetrum. Line 2 indicates lesser arc injuries, which occur through the direct ligamentous structures surrounding the lunate. Line 3 indicates translunate arc injuries, which occur through the osseous lunate.

arc injury should be directed toward the reduction and fixation of the lunate, with concurrent repair of any coincident lesser arc or greater arc dysfunctions.

Cases involving translunate arc injuries are typically the result of high-energy trauma. Consequently, these injuries are more severe, more difficult to treat, and are more likely to have a bad prognosis. There is potential difficulty in achieving satisfactory lunate reduction and fixation in the presence of coincident lesser arc and/or greater arc perilunate injury.

REFERENCES

1. Johnson RP. The acutely injured wrist and its residuals. Clin Orthop Relat Res 1980;149:33–44.
2. Mayfield JK. Patterns of injury to carpal ligaments. A spectrum. Clin Orthop Relat Res 1984;187:36–42.
3. Mayfield JK. Mechanism of carpal injuries. Clin Orthop Relat Res 1980;149:45–54.
4. Teisen H, Hjarbaek J. Classification of fresh fractures of the lunate. J Hand Surg 1988;13B:458–462.
5. Pourgiezis N, Bain GI, Roth JH. Volar ulnar approach to the distal radius and carpus. Can J Plast Surg 1999;7:273–278.
6. Garcia-Elias M, Geissler WB. Carpal instability. In: Green DP, Hotchkiss RN, Pederson MD, eds. Green's operative hand surgery. 5th ed. New York: Churchill Livingstone, 2005:591–602.
7. Herzberg G, Comtet JJ, Linscheid RL, Amadio PC, Cooney WP III, Stalder J. Perilunate dislocations and fracture-dislocations: a multicenter study. J Hand Surg 1993;18A:768–779.
8. Trumble T, Verheyden J. Treatment of isolated perilunate and lunate dislocations with combined dorsal and volar approach and intraosseous cerclage wire. J Hand Surg 2004;29A:412–417.
9. Adkison JW, Chapman MW. Treatment of acute lunate and perilunate dislocations. Clin Orthop Relat Res 1982;164:199–207.
10. Marsh AP, Lampros PJ. The naviculo-capitate fracture syndrome. Am J Roentgenol Radium Ther Nucl Med 1959;82:255–256.
11. Weseley MS, Barenfeld PA. Trans-scaphoid, transcapitate, transtriquetral, perilunate fracture-dislocation of the wrist. A case report. J Bone Joint Surg 1972;54A:1073–1078.
12. Hildebrand KA, Ross DC, Patterson SD, Roth JH, MacDermid JC, King GJ. Dorsal perilunate dislocations and fracture-dislocations: questionnaire, clinical, and radiographic evaluation. J Hand Surg 2000;25A:1069–1079.
13. Kuderna H. Frakturen und luxationsfrakturen der hand-warzel. Orthopade 1986;15:95–108.
14. Razemon JP. Fractures of the carpal bone with the exception of fractures of the carpal scaphoid. In: Razemon JP, ed. The wrist. Edinburgh: Churchill Livingstone, 1988:126–129.
15. Sasaki T. Lunate body fractures. J Jpn Soc Surg Hand 1991;8:635–639.
16. Conway WF, Gilula LA, Manske PR, Kriegshauser LA, Rholl KS, Resnik C. Translunate, palmar perilunate fracture-subluxation of the wrist. J Hand Surg 1989;14A:635–639.
17. Mason GC, Bowman MW, Fu FH. Translunate, perilunate fracture-dislocation of the wrist. A case report. Orthopedics 1986;9:1001–1004.
18. Takase K, Yamamoto K. Unusual combined scaphoid and lunate fracture of the wrist: a case report. J Hand Surg 2006;31A:414–417.
19. Noble J, Lamb DW. Translunate scapho-radial fracture. A case report. Hand 1979;11:47–49.
20. Vichard P, Tropet Y, Balmat P, Brientini JM, Pem R. [Reflections on 4 cases of ante-lunar carpal luxations]. Ann Chir Main Memb Super 1991;10:331–336.